Faculdade de Engenharia da Universidade do Porto

Recapitulating cardiac Ischemia-Reperfusion injury in human embryonic stem cell-derived cardiomyocytes in a microfluidic organ-on-a-chip device

José Dinis da Silva Faustino

17 de Junho de 2018

U.PORTO
FEUP FACULDADE DE ENGENHARIA
UNIVERSIDADE DO PORTO

MEB - MESTRADO EM ENGENHARIA BIOMÉDICA 2017/2018

A Dissertação intitulada

"Recapitulating cardiac Ischemia - Reperfusion injury in human embryonic stem cell-derived cardiomyocytes in a microfluidic organ-on-chip device"

foi aprovada em provas realizadas em 06-07-2018

o júri

Presidente Prof. Doutor Renato Manuel Natal Jorge
Professor Associado do Departamento de Engenharia Mecânica da FEUP - U.Porto

Doutora Diana Esperança dos Santos Nascimento
Investigadora do Instituto de Engenharia Biomédica - INEB - U. Porto

Prof.ª Doutora Perpétua da Conceição Pinto-do-Ó
Professora Auxiliar Convidada do ICBAS - Instituto de Ciências Biomédicas Abel Salazar da U. Porto

O autor declara que a presente dissertação (ou relatório de projeto) é da sua exclusiva autoria e foi escrita sem qualquer apoio externo não explicitamente autorizado. Os resultados, ideias, parágrafos, ou outros extratos tomados de ou inspirados em trabalhos de outros autores, e demais referências bibliográficas usadas, são corretamente citados.

José Dinis da Silva Faustino
Autor - José Dinis da Silva Faustino

Faculdade de Engenharia da Universidade do Porto

Faculdade de Engenharia da Universidade do Porto

Recapitulating cardiac Ischemia-Reperfusion injury in human embryonic stem cell-derived cardiomyocytes in a microfluidic organ-on-a-chip device

José Dinis da Silva Faustino

Dissertação realizada no âmbito do
Mestrado em Engenharia Biomédica

Orientador: Diana S. Nascimento

17 de Junho de 2018

Resumo

Atualmente, episódios de enfarte do miocárdio quando tratados com a devida urgência apresentam uma elevada taxa de sucesso. No entanto, a reperfusão de sangue no tecido resultante do alargamento da coronária (técnica de tratamento mais usada), apesar de minimizar a perda de cardiomiócitos, tem impacto negativo a longo prazo. O desenvolvimento de novos fármacos para tratamento da isquemia tem sido dificultado pela escassez de modelos *in vitro* capazes de recriar o musculo adulto. No sentido de responder a estes problemas, encontram-se em desenvolvimento modelos *in vitro* recorrendo à tecnologia de organs-on-a-chip, que tem como objetivo recriar os fenómenos e interações celulares que acontecem no organismo. No âmbito do coração, esta tecnologia tem utilizado cardiomiócitos derivados de células estaminais pluripotentes, minimizando a necessidade de recorrer a produtos celulares de dadores humanos. Contudo, atualmente a diferenciação de células estaminais em cardiomiócitos é deficiente uma vez que as células obtidas apresentam reduzida maturidade a nível metabólico e estrutural. Esta limitação prejudica a utilização destas células como modelos fidedignos do coração assim como a sua validade para o teste de novos fármacos. O plano de trabalhos aqui apresentado tem como objetivo desenvolver novos métodos de diferenciação de cardiomiócitos apartir de células puripotentes que promovam uma melhor maturação das células diferenciadas. Para tal foi desenhada uma abordagem inovadora que pressupõe a combinação de diferentes estímulos em níveis fisiológicos como forças mecânicas, nível de oxigénio e ainda substratos para a produção de energia. Paralelamente está a ser desenvolvido e otimizado um chip para a simulação *in vitro* de isquemia e reperfusão, onde mais tarde, poderemos testar os cardiomiócitos adultos num cenário de doença.

Abstract

Nowadays episodes of myocardial infarction when treated with due urgency, show a high success rate. However, reperfusion of blood on tissues, as a result from coronary elongation techniques (most common treatment technique), despite minimizing cardiomyocyte loss, has a long-term negative impact. The development of new drugs for the treatment of ischemia has been hampered by shortage of *in vitro* models capable of re-creating the adult muscle. To respond to these problems, novel *in vitro* organ-on-a-chip technologies have been developed, aiming at recreating cellular interactions observed in the organism. Concerning the heart, this technology has been using cardiomyocytes derived from pluripotent stem cells, minimizing the need to resort to cellular products from human donors. However, current differentiation of stem cells in cardiomyocytes is yet deficient, as obtained cells show reduced metabolic and structural maturity. This limitation impairs the use of this cells as bona-fide heart models as its validity for testing new drugs. The main goal of the work plan herein presented is to develop a new differentiation method to obtain fully mature cardiomyocytes from pluripotent stem cells. For that, we designed an innovative approach that combines the use of different stimuli at physiological levels such as mechanical forces, oxygen levels and even substrates for energy production. In parallel, a chip is being developed and optimized for an *in vitro* simulation of ischemia and reperfusion, which can be combined with the mature cardiomyocytes to mimic the disease scenario *ex vivo*.

Agradecimentos

Firstly, I want to thank every member of the Applied Stem Cell Technologies group for most importantly the great treatment given to me since day one, for creating comfortable working atmosphere, for the proper introduction to Dutch culture and as well for the help whenever it was asked, a sincere thank you Ingrid, Andries, Verena, Kim, Simone, Yusuf, Heleen, Wesley, Pritam, Sanders, AnneMarie, Renate, Oumaima, Thomas and Peter.

I would like address special thanks to my daily supervisor Rolf Slaats for all the patience and support, as well availability for the scientific discussions and non-scientific talks.
It is a great pleasure to acknowledge the chairman Prof. Robert Passier for providing me this opportunity to develop my ideas and grow as a scientist in a highly stimulative environment.

Gostava de dirigir também uma palavra especial de apreço aos "Tugas do AST" pelo companheirismo e ajuda independentemente da posição que ocupavam, por isso um obrigado especial ao Marcelo e Aisen, assim como às meninas Andreia e Lara.

À professora Diana S. Nascimento deixo um agradecimento especial, apesar da distância revelou sempre preocupação com o projeto e bem-estar pessoal, tendo sido indispensável na reta final para entrega desta tese. Por isso um muito obrigado.

Pais, Té e Mel, as saudades foram muitas mas obrigado por estarem sempre quando foi preciso.

À minha namorada Stephanie… O que quer que dissesse não ia ser suficiente… Mas também não preciso de dizer nada, tu sabes! Obrigado

"Esforço, Dedicação, Devoção e Glória", 1906
"Effort, Dedication, Devotion and Glory,", 1906

Índice

Figure List

Table List

Abreviations

ATP- adenosine triphosphate

BMPs- bone morphogenetic proteins

CM- cardiomyocytes

CO_2- carbon dioxide

CPC- cardiac progenitor cell

CPT1β- carnitine palmitoyltransferase1B

CSC- cardiac stem cell

D- day

ECM- extra cellular matrix

ESC- embryonic stem cell

FA- fatty acid

FACS- fluorescence-activated cell sorting

Glc- glucose

GLUT- glucose transporter

HADHB- hydroxyacyl-CoA dehydrogenase trifunctional multienzyme complex subunit beta

hESC- humans embryonic stem cell

HK1- hexokinase 1

HK2- hexokinase 2

IGF- insulin growth factor

iPSC- induced pluripotent stem cell

I/R – ischemia reperfusion

MEF- mouse embryonic fibroblast

MYBPC3- myosin-binding protein C

OXPHOS- oxidative phosphorylation

O_2- oxygen

PDMS- polydimethylsiloxane

PDMS- polydimethylsiloxane

PDK1- pyruvate dehydrogenase kinase 1

PGC-1α- peroxisome proliferator-activated receptor gamma coactivator 1-alpha

PLN- phospholamban

PPARα- peroxisome proliferator-activated receptor alpha

PSC- pluripotent stem cells

q-PCR- quantitative real-time polymerase chain reaction

RNA- ribonucleic acid

ROS- reactive oxygen species

SC- stem cells

SEM- standard error of the mean

SERCA2- sarco-endoplasmic reticulum Ca2+-ATPase

SCNT- somatic nuclear transfer

1. Introduction

1.1 - Cardiac ischemic disease

1.1.1 - Heart physiology

The first organ to become functional during mammalian development is the heart. Heart size is tightly controlled to secure functional blood flood[1], being regulated by organ-intrinsic mechanisms but also extrinsic chemical and mechanical factors. Heart growth is separated in two phases, during fetal grow is achieved by hyperplasia, by cardiomyocyte (CM) proliferation[2], while after birth it grows mainly by hypertrophy[3]. CM proliferation during development is controlled by several growth factors such as insulin-like growth factors (IGFs), bone morphogenetic proteins (BMPs), Wingless-related integration site (Wnts) and neuregulins[4]. After birth CM complete the maturation process which is paralleled by an arrest in the cell cycle.

The heart is comprised of diverse muscle and nonmuscle cell lineages: atrial and ventricular CMs, endocardial cells, valvular components, fibroblasts, conduction system cells, smooth muscle and endothelial cells[5]. During cardiogenesis these different cell types are derived from distinct embryonic progenitor populations. The working force of the heart is provided by the CMs, which are differentiated cells with highly developed cytoskeleton (sarcomere system) and great metabolic capacity. CMs occupy most of the heart volume, despite not being the most abundant cell type[6].

1.1.2 - Ischemia-Reperfusion

Ischaemic heart disease is a major burden in Western world. Cardiovascular diseases associated with ischaemia include myocardial infarction, stroke, pulmonary arteriole hypertension[7] and coronary heart diseases. The cardiac injury during acute myocardial infarction results from ischemia and subsequent reperfusion. Myocardial ischemia occurs on a distal region to the occlusion of an epicardial coronary artery. The interruption of coronary blood flow leads to an inability of the myocytes to maintain steady state cellular metabolism attributable to

lack of oxygen and nutrients [8]. Thus, infarct size is a defining factor of long-term mortality and chronic heart failure, thus therapeutic intervention to limit the extent of necrosis during infarct episode has great individual and socioeconomic value. The level of ischaemic injury and the transition from reversible to irreversible damage is time dependent. As reperfusion is not quickly re-esteblished on the hypoperfused myocardium, this tissue becomes necrotic. Even though reperfusion is crucial to partially retrieve the myocardial tissue affected, reperfusion can also accelerate the loss of CMs that have been severely compromised. CM calcium (Ca^{2+}) loading is recognized as a major factor in acute ischaemia–reperfusion pathology, promoting cell death, contractile dysfunction and arrhythmic activity. As the heart has very limited regenerative capacity, the lost myocardium is replaced by fibrous scar tissue. Since scar tissue does not contribute to myocardial contractility, if the scar is large, global left ventricular (LV) contractile function is impaired, resulting in progressive chronic heart failure. Besides that, the scar also offers a barrier to the natural propagation of electric impulse. This repair process contributes to a progressive reduction on left ventricular ejection fraction (LVEF), which explains why myocardial infarction is one of the main causes of chronic heart failure worldwide.

Deficit of oxygen during ischemia swings cardiac metabolism to anaerobic glycolysis, disrupting ATP generation by mitochondrial oxidative phosphorylation (normally 95% of ATP production in the heart), and thus reduces overall ATP availability[9]. This shift lead to accumulation of glycolytic products, including lactate and protons, lowering intracellular pH and subsequent stimulation of Na^+/H^+ exchange to export protons that drive to extracellular acidosis. The Na^+/H^+ exchange continues until the cross-sarcolemmal proton gradient is dissolute. In parallel with pH variations, this mechanism also increases intracellular Na^+[10] . In addition to Na^+/H^+ exchange other mechanism also contribute to a declined Na^+ efflux, such as Na^+/K^+ / Cl cotransport[11] and the opening of voltage-gated Na+ channels,[12]as well as the deterioration in the activity of the Na+/K+-ATPase[13]. A reduced Na+ gradient during ischaemia impairs activation of a myriad of important signalling pathways, [14]resulting commonly on CM death.

Infarct size may be easily limited by reperfusion, improving long-term myocardial function, reforming the healing pattern of the infarcted zone and reducing mortality. However, reperfusion triggers additional harm to the myocardium, known as reperfusion injury. Altogether, the damage inflicted on the myocardium is better defined as ischemia/reperfusion (I/R) injury. Risk-adjusted treatments in-hospital reduced mortality from 20% in the late 1980s to 5% in 2008 using reperfusion strategies and adjuvant pharmacology[14]. However, this drop-in mortality rates, have also resulted in augmented incidence of chronic heart failure.

Rebuilding of coronary flow flushes away extracellular the acidosis, and establishes a regular transsarcolemmal pH gradient. This exacerbates Na+ /H+ exchanger-mediated Na+ accumulation as proton export is recommenced, resulting in Ca^{2+} overload via reverse-mode Na+ / Ca2+ exchange[15]. Numerous CM pathologies are associated with an excess in intracellular Ca^{2+}[14]. For example, Ca^{2+} negligence in reperfusion is usually allied with systolic/diastolic dysfunction and arrhythmogenesis. Ca^{2+} can also overload and hasten CM death by multiple means. Hypercontracture and instigation of calpains, in mixture with cell swelling, cause sarcolemmal

rupture and non-programmed necrotic CM death. Amplified cytosolic oxidant environment and Ca^{2+} levels also promote mitochondrial Ca^{2+} loading, associated with opening of the mitochondrial permeability transition pore (mPTP) and programmed cell death by apoptosis.[16]

Morphological typical features of reperfused myocardial infarction are karyolysis (chromatin total dissolution), contraction bands, membrane disruption, mitochondrial swelling, disruption in CMs, accompanied by microvascular destruction, interstitial haemorrhage and inflammation.[17] The heart was thought to be devoid of CM turnover after birth, however during the first decade of the 21st century, different populations of cardiac stem cells (CSC), poised for activation in response to injury, have been identified in the adult myocardium. These cells here thought to be able to regenerate the myocardium after myocardial infarction and were often tested in murine models of myocardial infarction. CSCs are gathered together and coupled with the adjacent cells through the expression of gap and adherents junctions. Preservation of the undifferentiated state of CSCs appear to be sustained by adherents junctions. CSCs can also differentiate towards the endothelial and smooth muscle lineage. Altogether, despite heart damage cannot always be repaired intrinsically, this new insight opens new opportunities to different approaches in the prevention and treatment of ischemic pathologies.

1.2 - Cardiomyocyte can be differentiated *in vitro*

1.2.1 - Cardiomyocyte structure

CMs, are tubular shaped with diameters around 10 μm and 25μm with respective length between 30 and 100μm[18]. Due to the high metabolic behaviour in order to produce adenosine triphosphate (ATP), CMs have high number of mitochondria's. These cells carry central nuclei and the cell also contain myofibrils organized in aligned sarcomeres through the cytoplasm[19] 10. CMs form dense cellular networks, strongly attached top-to-top through intercalate discs (mechanic connection) also communicating through hiat junctions (electric connection).[18] Sarcomeres are multi-protein complexes forming basic units responsible for CM contraction. Sarcomeres are composed by two filament systems: thick filaments of myosin and thin filaments of actin, troponin and tropomyosin[18]. Sarcomeres are responsible for the CM striatum and could be divided in 4 microscopic distinct areas: 1) Z discs form the limit of each sarcomere; 2) I-bands containing actin and myosin filaments around Z disc; 3) an A-band is localized between two I-bands; and an 4) M line in the centre of sarcomere[19]

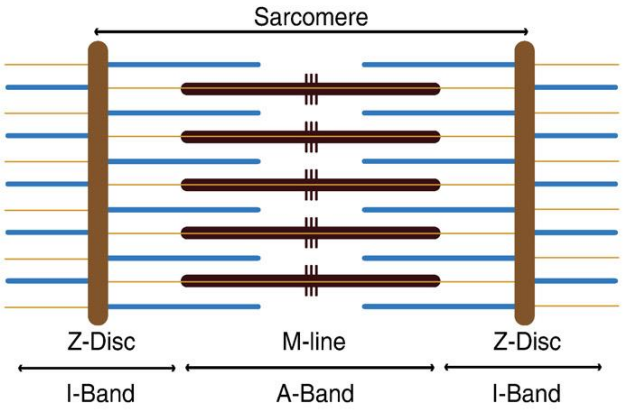

Figure 1.2.1.- "Schematic representation of the sarcomere. Sarcomeres are multi-protein complexes and the basic units of myofibrils."[19]

The size of each sarcomere is a determining factor for CM contraction strength . In physiological conditions varies between 1.6 and 2.4μm, being the overlap above of actin and myosin filaments optimal for lengths of 2 to 2.4μm[18]. The contraction/excitation of CM is promoted by the universal herald of intracellular signalling, calcium ions (Ca^{2+})[20]. Ca^{2+} is essential to cardiac electrical activity, activating directly myofilaments contraction[21]. Cardiac contractility and relaxation modulation by intracellular calcium levels is an indispensable mechanism to the increase of myocardial strength induced by stress hormones (adrenaline) which increase the uptake of calcium during action potential[20]. Excitation-contraction coupling describes the processes required for electric excitation of the myocyte until the contraction of the heart[21]. The sarcolemma is the muscle cellular membrane, and in CM is characterized by invaginations named T tubules. T Tubules, are opened to the extracellular space allowing ionic exchanges necessary to electric depolarization and repolarization of cells. In the cytoplasm associated with T tubules, exists an extended network of tubular ramification called sarcoplasmic reticulum (RS), being composed by terminal cisterns on the limit next to T tubules. Between cisterns and tubules exists regions of electronic density, responsible for the detection sarcolemma depolarization and enabling Ca^{2+} entry through channels type L. The combination between Ca^{2+} influx and liberation increases the concentration of free Ca^{2+} that binds to troponin C originating a transformation in the shape of troponin that leads tropomyosin to shift its position along the actin filament, thus allowing myofilament contraction between actin and myosin.

1.2.2 - From stem cells to cardiomyocytes

Human CMs used in *in vitro* experiments can be obtained from biopsies, or more recently, from stem cell differentiation into cardiac cells. When stem cells (SC) were discovered during the 60's of the past century, they were recognized as cells with self-renewal capacity, long term viability and multilineage potential.

Since then different SC or SC-like populations were identified on almost every tissue in the human body. Well-defined SC pool are associated with tissues where differentiated cells have

a short lifetime, for example the blood, epidermis and intestinal epithelium which are tissues with high cellular turnover and regenerative potential, contrasting with the heart, retina and spinal cord.[22]

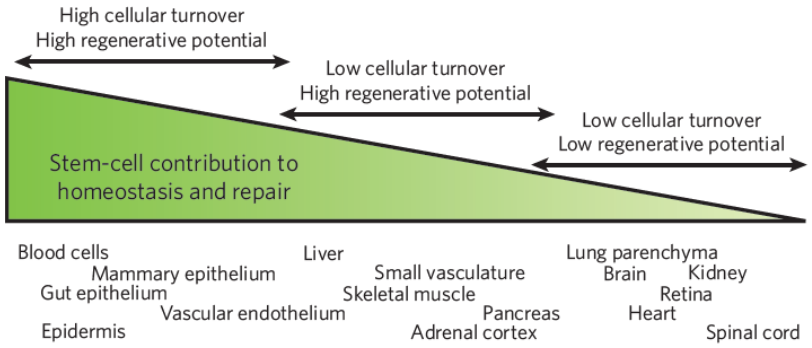

Figure 1.2.2. - Resident stem cells determine the turnover of the tissue.[22]

In contrast to tissue resident stem cells, embryonic stem cells (ESC) can only be obtained through direct extraction from early developmental stages from pre-implantation mouse and human embryos and maintained in culture as undifferentiated cells. Using nuclear reprograming on somatic cells, resulting from nuclear transference of somatic cells (SCNT) or with pluripotent stem cells (iPSC) technology is also possible to obtain stem cells. ESC are able to proliferate indefinitily *in vitro*. They are derived from the inner cell mass (ISM) of the developing embryo (blastocyst), 5 days after fertilization, and have the potential to develop derivatives of the three germ layers, even after a long period of culture. In 1981, Evans & Kaufman derived the first ESC line from the inner cell mass of blastocysts which were maintained *in vitro* resorting to embryonic feeder cells (MEFs) and medium containing fetal calf serum (FCS). In 1998, Thomson and colleagues shown that ESC could also be isolated from human blastocysts.

hESC present normal karyotype, express high levels of telomerase, express unique surface markers (e.g. SSEA-1/-3/-4 e TRA-1-60, TRA-1-81) that are not commonly expressed in other premature lineages or differentiated. ESC express high levels of telomerase activity. Telomerase is a ribonucleic protein that adds telomeric repeats on chromosome extremities and is involved in the maintenance of telomere length. Human differentiated cells do not express telomerase, their telomeres shrink through life and enter replicative senescence after a finite number of divisions. Germ lines and embrionic tissues have high levels of telomerase. The telomeric activity is the indicator of cell potential to proliferate, being the high level of telomerase expressed in hESC suggesting that their lifespan will exceed the one verified on somatic cells. Although, hESC can be identified by high nuclear/cytoplasmic ratio, alkaline phosphatase and specific cell surface markers. *In vivo* teratoma formation is considered the golden standard for pluripotency evaluation.

Blastocysts are not the only source of pluripotent ES cells. Pluripotent epiblast stem cells, known as epiSC, can be resultant from the postimplantation epiblast of mouse embryos [23].

Gene expression profiling showed that hESC are more like epiSC than to mouse ESC[24]. Pluripotent stem cells can also be derived from primordial germ cells, progenitors of adult gametes, which diverge from the somatic lineage at late embryonic to early fetal development [25]

Pluripotent cells can also be derived from reprogramming of adult somatic cells by transfer of the adult nucleus into the cytoplasm of an oocyte [26],[27] or by fusion with a pluripotent cell[28]. Decades later, the work of Yamanaka showed that skin fibroblasts can be reprogrammed to a pluripotent state using specific cocktail of factors, these cells were named induced pluripotent stem cells (iPSC). A mechanism reproducible of reversion into a pluripotency state. Some premises were used to sustain this discovery: pack of transcription factors seem to be always present in pluripotency state in ES cells *in vitro*; a set of active genes are active relative to one another, hipomethyled. Using reporter gene to identify the modify cells where introduced with retrovirus transduction 24 factors. Some of genes were able to revert the cells into a pluripotent state, guiding to more tests that narrowed the gene list to four essential factors: Oct4, Sox2, Klf4 e c-Myc. Later studies using the same technique reported other transcription factors Oct3/4, SOX2, Nanog, Lin28[28]. Reprogramed cells were like ESC, in terms of self-renewal capacity, differentiation potential, being able to give rise to cells of the three germ layers, and supported the information of teratomas *in vivo*.

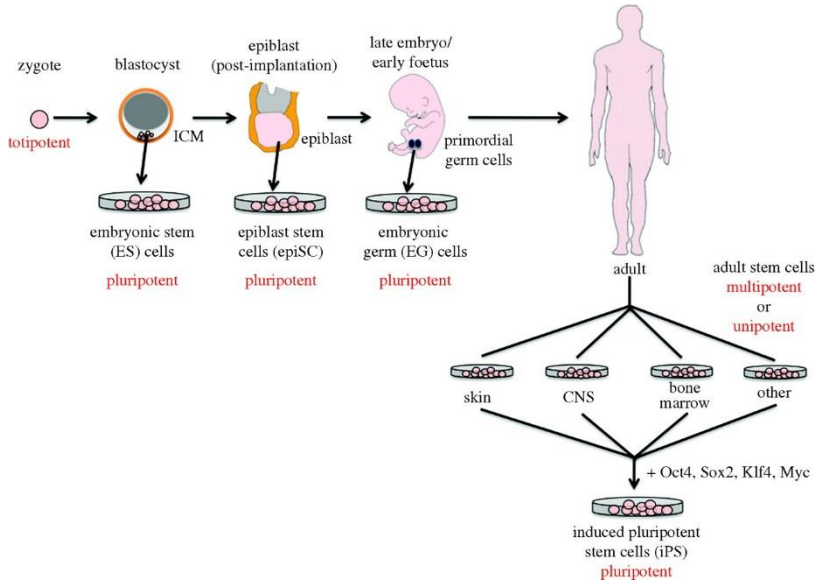

Figure 1.2.3. *"Origin of stem cells. Cells are described as pluripotent if they can form all the cell types of the adult organism"*[29]

The efficiency of *in vitro* differentiation of pluripotent stem cells into CMs is poor and differentiated cells are normally a heterogeneous mixture of various cell types[30]. The problematic of using pluripotent stem cells is the necessity to acquire pure populations of differentiated or committed cells, to circumvent the formation of teratomas[30]. The initial step during *in vitro* differentiation of CM from pluripotent cells, is stimulation of mesodermal lineages through activation of Wnt and nodal (TGF-ß) [31]. Cardiogenic mesoderm is then induced by

Mesp1, promoting development of mesoderm precursors of the cardiovascular lineage as well as repressing the expression of key genes regulating other early mesoderm derivatives[32]. The final stage of differentiation to CMs is the differentiation of committed cardiac progenitors to beating CMs, stimulated and controlled by factors such as Wnt11[33]. The identification of maturing CMs is commonly attained by confirming the presence of cardiac structural proteins such as α-actin, α-myosin heavy chain (α-MHC), BNP, islet-1140 or the cardiac isoform of Troponin-T (cTnT).[34]

1.3 - Cardiomyocyte maturation

CMs maturity is commonly evaluated based on various characteristics: 1) cell morphology and sarcomeric length, alignment, organization and abundance; 2) metabolism; and 3) calcium mechanism. Through the comparison between CMs at different ontogenic stages and CMs generated *in vitro*, it was possible to establish that current hPSC derived CMs are equivalent to late fetal CMs. Structurally speaking, human adult ventricular CMs displays a surface area of 10,000-14,000 μm^2 [35] and length-to-width ratio r of 7:1 to 9.5:1[36]. Even after cellular dissociation, the adult CM structure is commonly maintained due to the highly organized internal architecture. CM size and shape is functionally important, as an indicator of internal organization which is relevant for a variety of functional properties such as impulse propagation, action potential depolarization velocity, total contractile force and membrane capacity (directly related to cell surface area). The average length of a relaxed sarcomere is 2.0-2.2μm. The well-developed and abundant sarcomeres in adult CMs portrait myofibril perfect alignment being evident in electron microscopy images where the sharp, highly aligned organized Z-disc structures can be observed. The contractile stress, myocardial fibres force per unit area, is developmentally-regulated, having adult CMs more force than fetal counterparts. The active stress created by freshly harvested human ventricular CMs is >50 mN/mm^2 [37]. Action potential propagation is anisotropic as a result of the high concentration of gap junctions in the intercalated discs and low concentration at the lateral cell CM borders[38]. Adult CMs excitation-contraction coupling is intermediated mainly by calcium-induced calcium release, showing a positive force-frequency association when paced[39],[40]. Myosin heavy chain structural protein isoform and beta-myosin heavy chain (b-MHC), are predominant in adult ventricular CMs while the opposite is verified for alpha-myosin heavy chain (a-MHC)[41]. Other structural protein is MYBPC3 encodes for the thick filament associated protein cardiac myosin-binding protein C, a signalling node in cardiac myocytes that contributes to the maintenance of sarcomeric structure and regulation of contraction and relaxation[42].

During development, oxygen and nutrients requirements increase, as well the distance that they need to be transported. Hence, as development progresses blood flow rises, intensifying the hemodynamic loading on CMs resulting therefore in increased fibre length, contractile force

and stroke volume according to Frank-Starling mechanism. The latter is deceptive in human fetal heart from 10 to 15 week of gestation[43]. Increased Ca2+ sensitivity has been accredited to this mechanism, impacting specially at longer sarcomere lengths that induces an increase in the force of contraction [44].

Fetal CMs have an average length of a sarcomere in a relaxed state of 1.8μm and have a surface area ranging from 1,000–1,300μm^2 [45]. Fetal CM isolated from human foetus between 14 to 19 week, show a contractile stress of 0.4mN/mm^2 [46] whereas neonatal CMs generate a contractile stress of 0.8–1.7 mN/mm^2 [47]. Measuring with same experimental setting, neonatal CMs dramatically rise their contraction capacity as the contractility machinery matures, causing a two or threefold increase in strength compared to the fetal period. The immature asynchronous beating behaviour of early fetal CMs is related to the randomly distributed proteins along the cell membrane as CMs at this stage still lack of distinguishable intercalated discs. Fetal CMs are also immature electrophysiological level. The depolarization velocity of fetal CMs ranges from a 6 to 50-fold lower, compared to adult CMs. Some maturation transformations are particularly evident during around birth as CMs switching from hyperplastic growth to hypertrophic growth [35],[48].

The similarity of hPSC-derived CMs to fetal CM stages of maturation, has been well docomentend at several levels. Sarcomeres in hPSC-CMs display reduced contractile protein organization with very low myofibrillar density as shown by sarcomeric α-actinin staining[49], size wise they are also 25 to 30% shorter than in adult CMs and 6–11% smaller than in fetal CMs (1.6–1.7μm [50]. However, long-term culture (80–120 days) may increase the sarcomeres length of the hPSC-CMs to the same size of fetal CMs. hPSC-CMs have less defined sarcomeric structures and reduced organization comparatively to fetal CMs[51][46]. Sarcomeres underdevelopment relates to the lack of organization that support different myofilament regions[52], creating unaligned Z-discs of variable width[53], reduced quantity and an uneven distribution throughout the cell, also being sarcomeres more concentrated in the perinuclear region[54]. Proteins responsible for sarcomeres contraction can be detected in PSC-CMs, nevertheless at a much lower level of expression comparing to adult CMs. During fetal stages α–MHC is the predominant isoform. Long-term culture, also improves hESC-CMs machinery organization despite not contributing to t-tubule[49] or M band formation[50], demonstrating that functional maturity was not reached. Immature asynchronous beating observed in hESC-derived CMs is related to the randomly distributed proteins along the cell membrane with lack distinguishable intercalated discs, and has been reported to range from 21 to 84 beats per minute. Measured with same experimental setting, the contractile stress of seeded fetal cells aged between 14 to 19-week CMs was 0.4mN/mm^2 [46] and 0.15–0.30mN/mm^2 for hPSC-CMs[55]. The calcium kinetics of hESC-CMs is similar to fetal CMs with low amounts of CASQ2, RyR, SERCA, and L-type calcium channels, possessing little SR function and t-tubules, relying mostly on trans-sarcolemmal calcium intake to rise intracellular calcium[49]. SERCA2 gene encodes Ca(2+)-ATPases, which are intracellular pumps located in the sarcoplasmic or endoplasmic reticula of muscle cells, catalysing the hydrolysis of ATP coupled with the translocation of calcium from the cytosol into the

sarcoplasmic reticulum lumen while phospholamban (PLN) encodes a key regulatory protein of cardiac diastolic function, modulating calcium re-uptake during muscle relaxation, so that plays an important role in calcium homeostasis in the heart muscle. Previously mentioned genes have enhanced expression on mature CMs[56].

CMs in the myocardium are subjected to three types of persistent mechanical stimuli that influence their development: stretch during heart filling, hemodynamic compression from blood circulation and active self-induced cytoskeletal contractions[57]. Cellular mechanotransduction is the mechanism by which cells convert mechanical stimuli into biochemical reactions.[58] *In vitro* cells tend to sense and respond to external forces, changing the assembly of molecules promoting an alteration in their function. The structures mostly affected are the cytoskeleton, surface processes, adhesion proteins, nuclear lamina and stretch-activated channels.[58] Cell cytoskeleton is the basic support to cellular organelles, providing the physical edifice of cells. It comprises a network of actin and tubulin filaments and tubules that are disseminated over the entire cytoplasm. Any force transfers from inside (contraction) or outside (mechanical pressure) the cell leans towards it. The cytoskeleton has been shown to be a tensegrity (tensional integrity) structure with elements under compression (microtubules) that are held together by elements under tension (microfilaments, intermediate filaments).[59] To detect extracellular "aggressions" cells developed protrusions, as primary cilia, including itself receptors and channels that can be triggered through the physical activation of these processes by external forces[60]. This "aggressions" are promoted by the attachment to the extra cellular matrix (ECM) and to other cells. To promote this connections in cell-ECM contact exist specialized membrane proteins (integrins)[61], as well for cell-cell contact (cadherins and gap junctions)[62],[63]. Biochemical changes resultant from mechanical stimuli can have immediate impact, at the cell membrane via conformational variations in membrane proteins, also transmitted to the cytoskeleton inside the cell. This interactions on CMs were proved to influence functional characteristics as impulse propagation[64],[65], contractile force output and excitation-contraction coupling[66]. *In vivo* mechanotransduction signalling permits the cytoskeleton to remodel in reply to changes in the load on the myocardium, altering CMs aspect ratio and sarcomere density in an attempt to maintain cardiac output, proving the role of cytoskeletal architecture on responses to extracellular mechanical stimuli[36], [64], [67], [68]. The long-term impact involves changes in gene expression, happening due to downstream reactions from mechanical stimuli[69]. It is also thought that some direct force is applied in the nucleus as a result of the direct connection between nucleus chromatin and lamina with the cytoskeleton, this way transferring forces to the nucleus[70]. During heart development, CMs experience morphological changes as they advance toward the adult phenotype[53], organizing into laminar sheets of muscle tissue[71]. Cytoskeleton actin remodelling in confined regions of CMs, being identified as modifier of cell shape that drive looping of the heart tube during embryonic development [36]. Following a Natural Engineering philosophy, *in vivo* mechanical environment of cells can be replicated *in vitro*, including substrate stretching to which cells are attached, shear stress caused by fluid flow over cells, compressive forces (hydrostatic pressure), substrate

stiffness altering and shifting substrate topography. Additional techniques such as traction force microscopy, micropillar arrays, magnetic tweezers, optical tweezers, and atomic force microscopy have been employed along with force quantification to comprehend mechanotransduction mechanisms[72]–[74]. CMs are uninterruptedly subjected to cyclic mechanical strain made by rhythmic heart beating. Adult CMs begin to dedifferentiate when they are placed in 2D culture without mechanical loading. Zimmerman, Eschenhagen and colleagues proved that seeding immature CMs in suitable 3D matrix and exposing them to mechanical stress will enhance their maturation[75].

The correlation between physiological levels and the standard values used nowadays to culture cells need an approximation, specifically the case of atmospheric gases and stem cells and respective differentiation into specific cell lines, for example what is consider hypoxic environment, are the pO_2 values, 3–5%, required to maintain the full pluripotency of mammalian ES cells[76]. It was demonstrated that human ES cells proliferate have a similar development when cultured at 3–5% O2 as they do under 21% pO_2, yet, analysis of morphology and the loss of stem cell markers such as stage-specific embryonic antigen (SSEA) and the transcription factor OCT4, was substantially reduced. Physiologically normoxic conditions for embryonic or adult cells fluctuates broadly, between 2% (14.4 mm Hg pO_2) and 9% (64.8 mm O_2 Hg). Previously to the formation of circulatory system, human development occurs in a relatively O_2-poor environment (3%-4% O_2)[77]. To assure acceptable O2 demand, foetuses present diverse strategic variations as higher heart rate, higher haemoglobin concentration and a large surface area for gas exchange in the placenta[78]. Organisms have mechanisms at molecular level to preserve O2 homeostasis, hypoxia-inducible transcription factors (HIFs), the environmental sensing mammalian target of rapamycin (mTOR) and the endoplasmic reticulum (ER) stress response[79]. Placentation is the initial step of development of the embryo on mammalian development and it occurs in a low oxygen ambient. At this stage there is no blood flow from the mother into the emerging placenta until the 3rd month of gestation, essential due to tissues immaturity to protect themselves against oxidants[80]. Entering the second trimester maternal flow is set, after the collapse of endovascular trophoblast plugs rising the placental pO2 to values above 50 mmHg.[81] The placental pO_2 keeps this values until birth. pO_2 should be ponder as a developmental morphogen that influences cell fate in a similar way to the more traditionally recognized gradients of secreted growth factors. Adult CMs produce their energy mostly from oxidative metabolism, with 90% of their acetyl-CoA created from oxidation of fatty acid[82]. Fat provides 60% of energy while anaerobic metabolism accounts for less than 1%. Also, in adult CMs glycogen lodges 2% of cell volume[83] and mitochondria's 20%-40%[84]. Cardiac tissue suffers a developmental conversion from using glycolysis into fatty acid based oxidative phosphorylation (OXPHOS)[85]. In order to support directly the energy necessities (ATP) for cell contraction, mitochondria with well distributed lamellar cristae are crowded below the sarcolemma or along myofibrillar proteins such as sarcomeric α-actinin to form functional energetic units[37]. Embryonic and fetal CMs create their ATP mainly through glycolysis, being oxidative metabolism eligible for less than 15% of the total acetyl-CoA production[53]. Also, in fetal CMs glycogen

ocuppies 30% of the cell volume[86] and mitochondria account for a small fraction of cell volume. Mitochondria are dispersed across cytoplasm and have the morphology of a vesicle because of the absence of complete cristae in the inner mitochondrial membrane[87]. Birth brings metabolic pressure because there is an increase in contractile function, cells experience fatty acid as a substrate for energy, and oxygen levels rise rapidly. This phenomenon triggers neonatal CMs to change to oxidative metabolism with an increase in mitochondria size and amount, development of cristae, and a more ovular-shaped mitochondria morphology[88]. Fetal mitochondria are randomly distributed, mostly in the perinuclear region (by this time they are mostly needed in this area, due to highly hyperplastic behaviour of fetal CMs requiring lots of cell energy to sustain the nuclear activity) also containing less dense myofibrillar structures. Metabolically hPSC-CMs are identically to fetal CMs being predominantly glycolytic and expressing oxidative phosphorylation genes although at low levels. Immature CMs seem to rely on glycolysis and lactate oxidation (majority of myocardial oxygen consumption[89], as a source of energy, with mitochondrial oxidative metabolism from fatty acids a minor contributor.[90] Lactate production from glycolysis (accumulated from pyruvate degradation) exists even in the presence of adequate levels of oxygen. Mature and differentiated CM possess increased mitochondrial oxidative capacity, with fatty acid B-oxidation the main energy supplier. Fatty acid (FA) handling is a fundamental metabolic feature for mature CMs the transition is supported by genes like carnitine palmitoyltransferase1B (CPT1β), responsible for the import into the mitochondria of long-chain fatty acyl-CoAs, peroxisome proliferator-activated receptor alpha (PPARα) , FA concentration transducer working as a member of the nuclear receptor family of ligand-activated transcription factors that regulate gene expression and hydroxyacyl-CoA dehydrogenase trifunctional multienzyme complex subunit beta (HADHB) responsible for mitochondrial trifunctional protein, which catalyses the last three steps of mitochondrial beta-oxidation of long chain fatty acids. However, developed CMs diet is ‘‘omnivore’’, meaning that if necessary, they are able to oxidize glucose, lactate, ketones, and amino acids to produce energy[91],[92].Catabolic pathways of different energetic substrates, converge on acetyl-CoA production which is further used for ATP production[93]. The cardiac metabolism is known to be extremely flexible in using different substrates depending of their availability. This kinetics is maintained by hexokinases responsible for the first step in most glucose metabolism pathways, phosphorylating glucose to produce glucose-6-phosphate. Hexokinase 1 (HK1) is the isoform ubiquitously expressed in most tissues, whereas hexokinase 2 (HK2) is the main form found in skeletal muscle. Kinetics is also impacted by pyruvate dehydrogenase kinase 1 (PDK1) playing a key role in regulation of glucose and fatty acid metabolism via phosphorylation of the pyruvate dehydrogenases regulates metabolite flux through the tricarboxylic acid cycle, down-regulating aerobic respiration what inhibits the formation of acetyl-coenzyme A form pyruvate. Glucose transporters (GLUTs) on CMs have isoforms one and four as the most abundant. GLUT1 is mainly localized on plasma membrane, being responsible for a significant component of basal cardiac glucose uptake, while GLUT4 is mostly present in the intracellular vesicles at resting stages, and is translocated to the plasma membrane upon insulin stimulation. GLUT1 is predominant in

the embryonic and neonatal heart and GLUT4 is upregulated after birth while GLUT1 is down-regulated, subsequently GLUT4 is primary glucose transporter on mature CMs. [94]

Metabolic alteration occurs only after birth (birth shock), when oxygen levels are abundant[85]. Subsequently to birth, foetus blood levels of lactate decrease from 5–7 mM to approximately 0.5 mM in the adult circulation[95], while the levels of free fatty acids are very low in the fetal circulation, less than 0.1 mM, increasing immediately after birth to levels between 0.2–0.4 mM[95],[96] Notwithstanding this increase, fatty acid oxidation rates are kept low in the immediate neonate period, providing less than 15% of the cardiac ATP demands, thanks to an inhibition of mitochondrial fatty acid uptake[97]. The behaviour of CMs is responsive to the environment and energy capacities. Developing CMs proliferate in a relative low oxygen (3-5%) environment in the womb[98] and the metabolic phenotype provides the biosynthesis of cellular lipids, amino acids, nucleotides, and other macromolecules, all indispensable to produce enough material to form viable daughter cells.[99], Glycolytic metabolism seems to facilitate the maintenance of pluripotent and proliferative states.[90] The contractile capacity of mature CMs is generated through ATP production by OXPHOS. Increased mitochondrial oxidative capacity on CMs seems to be a mark of the switch to a more terminally differentiated state[59]. Mitochondria are responsible for producing more than 95% of the ATP used by CMs. If ATP production is aborted, the human heart is only capable of beating for few seconds since CM storage is minimal[100]. The contribution of glucose to energy production is very small, with the majority of energy being derived from fatty acid oxidation. Nevertheless, glucose is very important among myocardial substrates since it can give a small quantity of ATP through substrate-level phosphorylation during glycolysis, which occurs in the in the extra-mitochondrial compartment. This is crucial in ischemic conditions where oxygen levels are low[101] . Conversion from anaerobic glycolysis to mitochondrial oxidative phosphorylation guides the differentiation of ESC to CMs.[90] Such mechanisms are involved in regulation of both glycolysis and oxidative metabolism in undifferentiated stem cells verifiable also during cardiogenesis in the embryo *in vivo*, the transition from the immature metabolism into the mature metabolism is secured by a set of genes being PGC-1α an excellence marker for this phenomenon. Catabolic pathways of different energetic substrates, converge on acetyl-CoA production which is further used for ATP production[93]. The cardiac metabolism is known to be extremely flexible in using different substrates depending of their availability. Yet, metabolic immaturity of hESCs-differentiated CMs was verified by our group, revealing a fetal like metabolic behaviour. This phenomenon is also observed in *in vitro* cell cultures where high concentration of glucose is used. In this scenario cells generate energy through aerobic glycolysis instead of mitochondrial oxidative phosphorylation (OXPHOS), even though sufficient oxygen is present. For the first time observed in cancer cells, this event was designated as the Warburg effect[102].

The metabolic immaturity of CMs as revealed in both low or high O_2 setups cells always prefer to use glycolysis, being shown in some cases with only 0,1% of O_2, the cells can survive when they were expected to die. To mimic *in vitro*, the cardiac *in vivo* environment, and get

valid cells to use in further studies, diverse groups are using glucose deprived medium supplemented with galactose to trigger the use of OXPHOS metabolism. Although this metabolic swift has been observed, the underlying mechanisms are yet to be revealed. Some reports suggest relates with galactose handling by the cell i.e. the rate at which galactose is metabolised is much slower than glucose. Initially ATP is used to convert glucose to glucose-6-phosphate, while galactose-1-phosphate is theoretically not converted directly and passively to glucose-6-phosphate, turning the conversion slower. It requires the uridyltransferase to swap the galactose-1-phosphate with glucose-1-phosphate, which is then mutated to glucose-6-phosphate (Leloir pathway). This uridyltransferase requires UTP, which is synthesized from UMP using two ATP molecules (UMP->UDP->UTP). This is essentially where the extra ATP usage comes into play because with glucose transferase or UTP are not required. Production of pyruvate via glycolytic metabolism of glucose profits 2 net ATP, while the production of pyruvate via glycolytic metabolism of galactose yields has no ATP profit[102]. Therefore, cells are forced to use glutamine (highly abundant in culture media) and shift towards aerobic metabolism, resulting in a rise in the oxygen consumption rate compared to cells grown in glucose media[103],[104]. This way, the fact that galactose is carried into the cell at a slower rate than glucose, its conversion also takes longer, makes it a kinetic phenomenon as well. Altogether, galactose limits the carbohydrate flux into a cell, which enables the cell to adapt and utilize OXPHOS more regularly[103], [105]–[107] Reitzer et al. suggested that glutamine provides energy by aerobic oxidation from the citric acid cycle metabolism when carbohydrate are used in the culture medium is galactose[107]. Gohil et al. showed that human MCH58 skin fibroblasts cultured in glucose derive ATP from both aerobic glycolysis and mitochondrial glutamine oxidation. On the other hand, when cells are cultured in galactose they have a five to six-fold decrease in the extracellular acidification rate (ECAR), which means that there is a decrease in glycolysis. Additionally, a twofold increase in the oxygen consumption rate (OCR), consistent with a shift to glutamine oxidation was also observed. Via a mixture of ß-adrenergic stimulation (isoproterenol) and fatty acid supplementation to mimic post-natal developmental processes[108] our group was able to increase mitochondrial expression of enzymes of the electron transport chain complexes I to IV on cells supplemented with galactose and fatty acid. Nevertheless, the levels of expression are still lower than in adult CMs.

1.4 - Organ-on-a-chip technology

Organs-on-a-chip is a recent technological development with the potential to address different problematics. Concerning preclinical drug testing, the present golden standard is to first test drug *in vitro* before proceeding to animal models (*in vivo*). Besides being extremely expensive, labour-intensive and ethically contentious[109], animal testing habitually lacks predictive value[110], which is demonstrated by the large percentage (88%) of drugs eventually

failing in clinical trials[111]. The lack of predictive value can be attributed to the differences in pathophysiology between humans and genetically modified animal[112]. Variations occur in species-to-species expression profiles of transporter proteins[113] and in the electrophysiology of the heart muscle[114] . In order to surpass interspecies differences, human cells can be used in *in vitro* tests, however, these models are too simplified to authentically replicate the micro-environment of a tissue. In addition, cells in culture, in the absence of the native environment, tend to lose their specific tissue physiology[115]. Organ-on-chip models have the capacity to resolve some of these limitations[115]. They contain micrometre-sized channels in which cells can be cultured, allowing the precise control of the culture environment, trying to simulate the microenvironment of a certain organ by tuning mechanical, biochemical and geometrical aspects, resulting in a more predictive outcome.[115] Organs-on-chips can be engineered in such a way that they allow direct measurements of organ function as well as pharmacokinetics and pharmacodynamics, assisted by high-throughput mechanisms[116]. The ultimate goal of this technology is to create a natural engineering device, mimicking functional units of a certain organ rather than a complete organ, in order to work out a realistic but simple *in vitro* models[116]. Organ-on-chip devices created a big suspiciousness in the beginning. However, several proof-of-principle studies such as lung-on-a-chip[117], bacteria-inhabited gut-on-a-chip[118] and the atherosclerosis-on-a-chip[119], proved the robustness of this technology, namely for evaluating organ functions and physiological responses to stimuli that were not be tested before *in vitro*.

2 - Material and methods

2.2.1 - Stem cell maintenance

Delta-N3 hESCs were cultured with Essential 8 Medium (Life Technologies) containing 50 Ul/ml penicillin/streptomycin (P/S, ThermoFisher) on 6 well-plates (Greiner) coated with Vitronectin (Life Technologies). The cells were incubated at 37°C in humidified air with 5% CO_2 and with 4%/21% O_2. Stem cells were passaged for subculture or differentiations at a time of high confluence without individual colonies connecting to eachother.

2.2.2 - Feeder-free monolayer differentiation of hESC to cardiomyocytes

Differentiation protocol was proceeded on 6 well-plates(Greiner) pre-coated with Matrigel (Corning). On day minus one (D-1) wells were seeded with 250 000 hESCs per well in E8 medium and cultured overnight. On day zero (D0), medium was replaced by BPEL medium (3 ml/well), plus growth factors by adding (to a final concentration) 20 ng/ml ACT-A (Miltenyi), 20 ng/ml BMP4 (R&D Systems) and 1.5 µM CHIR(Axon Medchem). On day 3 (D+3) medium was refreshed with the prepared BPEL + 50 µg/mL Matrigel (Corning) + 5 µM XAV 939 (R&D Systems), final concentrations. On days D+7, D+10 and D+14 medium was refreshed with BPEL medium without any additions. Cell dissociations for subsequent experiments were usually done at D+13.

2.2.3 - Preparation of BPEL medium

Please refer to table 1 in the appendix

2.2.4 - Matrigel well-plate preparation

Matrigel stocks (Corning) were kept on ice during procedure to avoid gelatinization. Matrigel Matrix GFR was diluted to a concentration of 83 ug/mL using serum-free medium (DMEM-F12) using ice-cold pipette tips. One millilitre of diluted Matrigel suspension was added per 6-well; the plate is then incubated for 60 minutes at RT before use, or stored at 4ºC with an additional mL of DMEM per well for later use.

2.2.5 - Hypoxia equipment

Biospherix Xvivo System was used in hypoxia experiments. The working chamber was set to 37ºC, variable O_2 percentage depending on the current work being executed and 5% CO_2. The incubation chamber used to expose cells to hypoxia contained a humidified, variable O_2 percentage depending on the current work being executed and 5% CO_2 atmosphere at 37ºC. Nikon eclipse TS100 microscope was used to image within the hypoxia system.

2.2.6 - Chip fabrication

The microfluidic chips were produced by polydimethylsiloxane (PDMS) by soft lithography. In short, silicon wafer moulds with SU-8 microstructures were designed and produced as described previously (van der Helm, Odijk et al. 2016). PDMS base and curing agent were mixed in a 10:1 wt/wt ratio (Sylgard 184 Silicone elastomer kit, Dow Corning, Midland, MI, USA). After degassing the mixture, the PDMS was poured onto the SU-8 patterned silicon wafer and cured for at least 3 hours at 67°C. The cured PDMS with channel imprints was then cuted in individual chip blocks. After that, four inlets (1.2 mm in diameter) were punched into the block. Dust was removed using Scotch tape (3M). Microscope slides were spin-coated with 1:10 PDMS mixture and cured at 67ºC for 60 minutes. PDMS block and spin-coated microscope slide were then covalently bonded by air plasma activation of the surfaces (50 W) for 40 s (Cute, Femto Science) and gentle assembly, followed by a post-assembly bake of 60 minutes at 67ºC, then were coated with 83 µg/mL Matrigel (Corning) or Vitronectin 5 ug/mL (Life Technologies). Chip dimension was approximately 26 mm x 26 mm, composed by 7 channels separated with a PDMS barrier with pores of 3µm every 10 µm, as demonstrated on figure 2.2.6.1. Channels dimensions were 8000 µm in length, 300 µm wide and 58 µm height. Inlets and outlets 1.2mm of diameter.

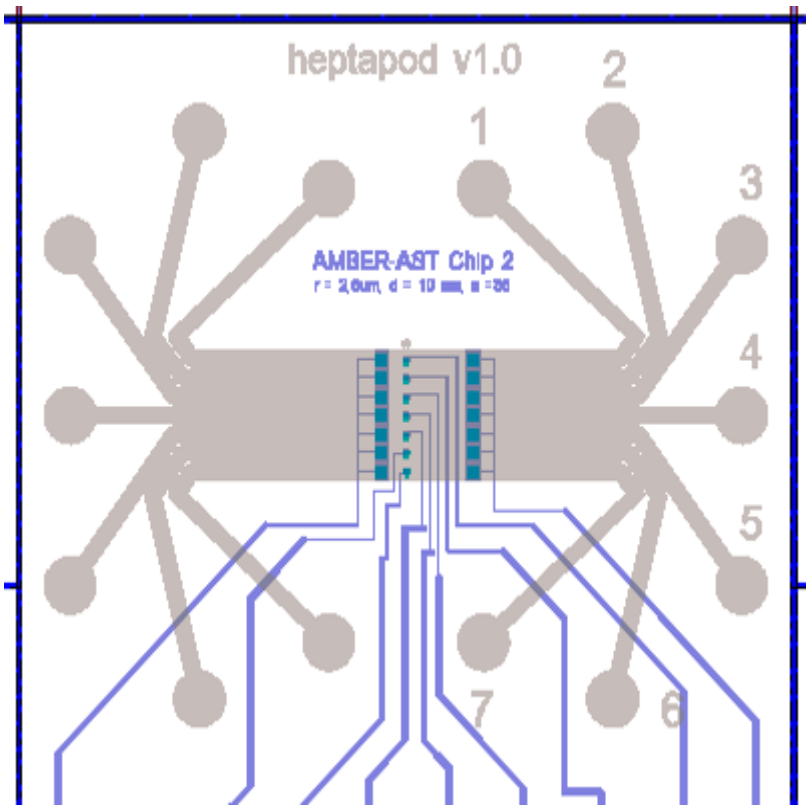

Figure 2.6.1. Illustrative image of chip design

2.2.7 – CMs seeding on chip

Chip channels were incubated with Matrigel solution as mentioned at point 2.2.4. Due to the small dimension it was only added 20µL per channel.

CMs dissociation (2.2.x). CMs counted on Neubauer Chamber (Sigma Aldrich), following a procedure of concentration or dilution, in order to produce a solution with 8× 10^6 cells/mL to 10×10^6 cells/mL after. In each channel through the inlets it was added 10µL of cell solution.

2.2.8 - RNA isolation

RNA isolation was performed with RNeasy Mini Kit (Qiagen) (74104). Kit protocol was followed, isolation was done at room temperature. The concentration and purity of RNA were measured by NanoDrop® ND-2000 spectrophotometer (Thermo Fisher Scientific), assuming as ideal ratio values of A260/A 280 between 1.8 and 2.1. Isolated RNA is kept on ice during handling and stored at -80ºC for later use.

2.2.9 - cDNA synthesis

cDNA synthesis from RNA isolation was performed using the iScript™ cDNA Synthesis Kit (Bio Rad, 1708891). Kit protocol was followed.

2.2.10 - qPCR

qPCR was performed on cDNA obtained using the Sensimix kit (GC Biotech) (QT615-20according to the manufacture instructions. Primers sequnces are detailed in Table 1.

Function	Full name	Symbol	Primer Name	sequence 5'-> 3'
Metabolic	Peroxisome proliferator-activated receptor alpha	PPARa	PPARa fwd	GCCTAAGGAAACCGTTCTGTG
			PPARa rev	TCCGACTCCGTCTTCTTGATG
	Glucose transporter type 4	GLUT-4	GLUT-4 fwd	GCCGGACGTTTGACCAGAT
			GLUT-4 rev	GGTGTTTCACCTCCTGCTCTA
	Glucose transporter type 1	GLUT-1	GLUT-1 Fwd	TCCACGAGCATCTTCGAGA
			GLUT-1 Rev	ATACTGGAAGCACATGCCC
	Hexokinase 1	HK1	HK1 fwd	GGACTGGACCGTCTGAATGT
			HK1 rev	ACAGTTCCTTCACCGTCTGG
	Hexokinase 2	HK2	HK2 fwd	CAAAGTGACAGTGGGTGTGG
			HK2 rev	GCCAGGTCCTTCACTGTCTC
	Lactate dehydrogenase B	LDHB	LDHB fwd	CTCCTGTGCAAAATGGCAAC
			LDHB rev	CCTAGAGCTCACTAGTCACAG
	Pyruvate Dehydrogenase Kinase 1	PDK1	PDK1 Fwd	CCGCTCTCCATGAAGCAGTT
			PDK1 Rev	TTGCCGCAGAAACATAAATGAG
	Hydroxyacyl-CoA Dehydrogenase Trifunctional Multienzyme Complex Subunit Beta	HADHB	HADHB Fwd	ACACTGTCACCATGGCTTGT
			HADHB Rev	CTGGCCAGAAGCAATCAAG
	Carnitine palmitoyltransferase 1B (fatty acids)	CPT-1b	CPT-1b Fwd	CAGGCGAGAACACGATCTTC
			CPT-1b Rev	GCGGATGTGGTTTCCAAAG
	Peroxisome proliferator-activated receptor gamma coactivator 1-alpha	PGC-1a (PPARGC1A)	PGC-1a Fwd	TGGTGCCACCACCATCAAAGA
			PGC-1a Ver	TCACCAAACAGCCGCAGACTG
Contraction Mechanism	Myosin heavy chain 6	a-MHC	MYH6 Fwd	GACTGTTGTGGCCCTGTACC
			MYH6 Rev	GGAAGGATGAGCCCTTTTTC
	Myosin heavy chain 7	b-MHC	MYH7 Fwd	GGAGTTCACACGCCTCAAAGAG
			MYH7 Rev	TCCTCAGCATCTGCCAGGTTGT
	Phospholamban	PLN	PLN Fwd	CTCACTCGCTCAGCTATAAGAAG
			PLN Rev	AGAGAAGCATCACGATGATACAG
	Myosin Binding Protein C, Cardiac	MYBPC3	MYBPC3 Fwd	GTCCCAAAGGGTCAAGCTCA
			MYBPC3 Rev	ATGCGCTCGTACTCAGATGG
	ATPase Sarcoplasmic/Endoplasmic Reticulum Ca2+ Transporting 2	ATP2A2	SERCA2 Fwd	ATGCACCTTGAGGACTCTGC
			SERCA2 Rev	ATCATGATGACCCGGATGCC

2.2.11 - Fluorescence imaging

Double reporter cell line, with GFP driven by an NKX2.5 promotor and an $\alpha-$ Actinin-mRubyII fusion protein was created in our group (unpublished data) through CRISPR mediated gene

editing. A reporter for α-actinin, a protein localized at Z-disc of microfilaments and analogous dense bodies, helping to anchor the myofibrillar actin filaments, enables imaging of sarcomeres. Imaged in a Nikon TE2000U (10x or 20x Nikon objective) or a EVOS FL (ThermoFisher) (respective objectives 10x and 20x).

2.2.12 - Dissociation of hESC-derived cardiomyocytes

CMs on the wells were washed with 2-3 ml PBS (Thermo Fisher). Next, it was added 1000 µl 1x or 10x TrypLE (Thermo Fisher) (depending on day after differentiation, older cells were harder to detach). Incubated for 10 min. Finally, it was added 4 ml BPEL medium to the cells to inactivate the TrypLE.

2.2.13 – Mitochondria staining

Mitochondria phenotype and location is addressed using MitoTracker® Deep Red FM (ThermoFisher) (M22426), far red fluorescent dye (abs/em 644/665 nm) that stains mitochondria in live cells. Final solution of 40nM. Cells were loaded with Hoerst (Sigma Aldrich) and MitoTracker Far Red (CMs, 40 nM, Invitrogen) in the above experimental buffer for 20 minutes, thenimaged in experimental buffer with a Nikon TE2000U, custom-built on-stage incubator to keep the plate in the proper experimental conditions, the objective was a NIKON CFI super fluor 40x /1.30 oil immersion objective or quantified by flow cytometry (2.2.14).

2.2.14 - Flow cytometry

Sony SH800S Cell Sorter, was used to obtain and quantify the different population of cells in a dish after a differentiation for further analysis of the mechanism promoting this differentiation. CMs were dissociated (2.2.x) from each well. Solution was centrifuged for 3min, 2400 RPM, and supernatant removed. Cells were resuspended on FACS buffer, and placed on FACS tubes after passing the strainer.

2.2.15 - Statistical analysis

Statistical analysis was performed using GraphPad Software. Error bars represent mean ± S.E.M. unless stated otherwise.

3. – Results

3.1. Embryonic pO2 levels support maintenance and recovery of cryo-preserved hESC.

Atmospheric levels of oxygen (21% pO_2) and conventional tissue levels of carbon dioxide (CO_2) (5% CO_2) are generally used as standard conditions for *in vitro* cell culture. However, previously to the formation of circulatory system, human embryonic development occurs in a relatively O_2-poor environment (3%-4% O_2)[77]. Aiming at adjusting hESC culture to physiological levels, we compared 4% pO_2 to standard 21% pO_2 conditions during hESC recovery after cryo-preservation. After thawing, hESC were routinely cultured in E8 medium which maintains cells in a pluripotent state[120]. After defrosting, hESC recovery at 4% pO_2 was slower, as shown by smaller and less abundant hESC colonies at passage 2(Figure 3.1.1. A and C). In fact, hESC at 4% pO_2 required the double of passages to attain a phenotype similar to 21% pO_2 (Figure 3.1.1. B and D) and usable for monolayer differentiation into CMs.

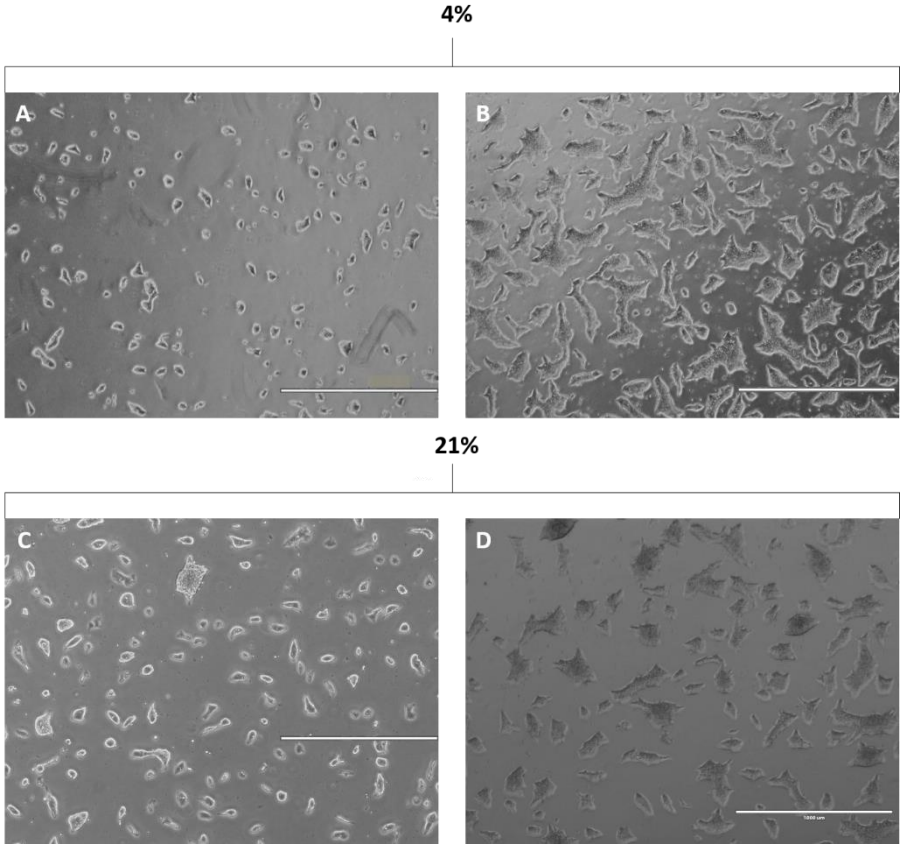

Figure 3.1.1. Representative brightfield images of hESC in culture at 4% and 21% pO_2. A and B- hESC maintained 4% pO_2 during 2 (A) and 8 passages (B). C and D- hESC maintained 21% pO_2 during 2 (C) and 4 passages (D). Scale bar, 1000µm.

3.2. *In vivo* pO2 levels support CMs differentiation from hESC.

Hypoxia is known to sustain pluripotency, thus, introducing embryonic physiological levels of pO2 may constitute a challenge for SC differentiation into specific lineages.

To determine which condition was most favourable to support CM differentiation from hESC, an experimental setup was established (Figure 3.2.1) for pairwise comparison of the introduction of 4% pO_2 at different culture stages. The standard culture condition at 21% pO_2 was compared with the use of 4% pO_2 during all culture stages (condition 4%) and the introduction of 4% pO_2 immediately after hESC passaging (day minus one (D-1) (condition 4%1), or on the next day (day zero (D0) (condition 4%2) (Figure 3.2.1).

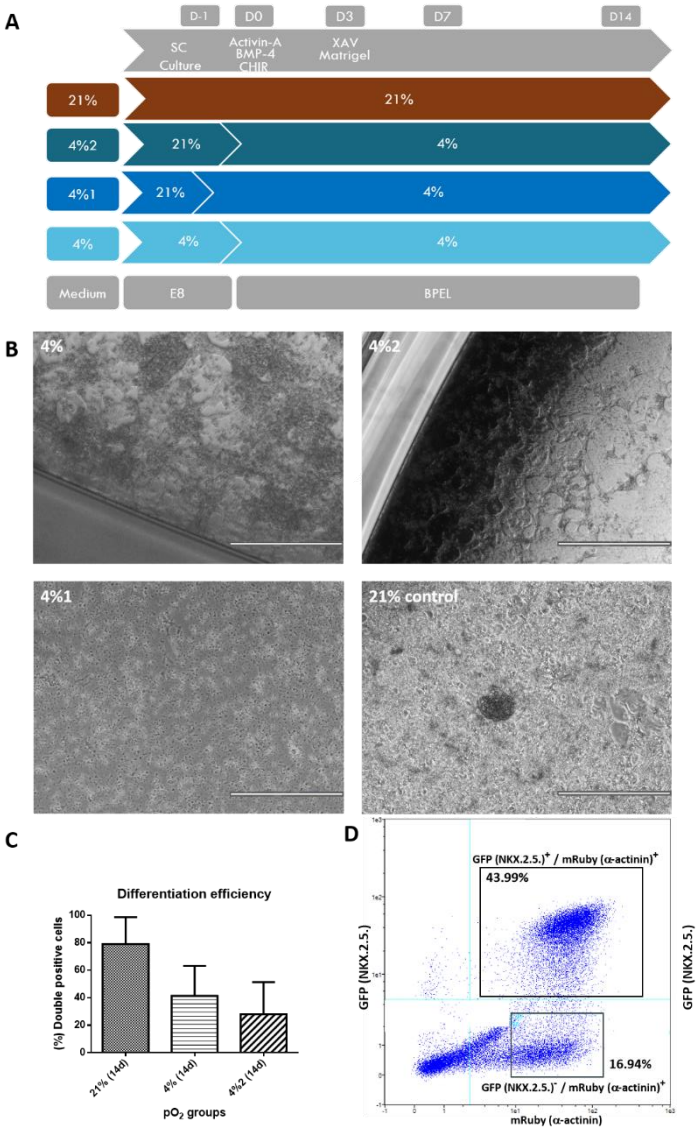

Figure 3.2.1. A- Diagram illustrating experimental physiological pO2 setup, level, 14 day procedure. 21% group (control), was always kept at all stages under 21% pO2; 4% group originated from 4% SC. 4%1 and 4%2 group have their origin on 21% SC. 4% group was always kept at all stages under 4% pO2, while 4%1 and 4%2 group were kept at this condition during 15 and 14 days, respectively. Small grey boxes indicated the day of culture (D-1, D0, D3, D7 and D14). Medium group indicates to what kind of medium cells were cultured, SC stage cultured in E8 and differentiation stage cultured on BPEL. Timeline of differentiation

factors added to medium presented on grey arrow. B- Representative brightfield images of differentiated CMs from the groups of the diagram A CMs in culture at 4% and 21% pO2. Scale bar, 1000µm. C- Different group differentiation efficiency of hESC derived CMs analysed through flow cytometry. The cells are divided per differentiation group. Control-21% group, 4% group and 4%2 group. Results presented as percentage (%) of cells GFP (NKX 2.5)+/mRuby (α-actinin)+ characteristic of CMs. Bars represent SEM.*P<0.05 vs Control; T-Test was used for all the parameters presented. D- Flow cytometry analysis of different experimental groups. Gating for GFP-NKX2.5. (y axis) and mRuby- α -actinin (x axis). Percentage related to to the two existing population GFP (NKX 2.5)+/mRuby (α -actinin)+ and GFP (NKX 2.5)-/mRuby (α -actinin)+. At least 60 × 10^6 cells were analysed per group.

Cardiac differentiation efficacy was initially assessed by the appearance of beating colonies and quantified through fluorescence analysis of the two reporters - GFP (NKX 2.5)$^+$/mRuby (α-actinin) – by flow cytometry. The 4%1 group failed to produce contractile CMs colonies (Figure 3.2.1 B and C) and therefore was removed from subsequent experiments. The conditions 4% and 4%2 produced contractile CMs (movie 1.1-1.2. and movie 2.1-2.2, respectively) with a low yield. Surprisingly, the obtained CMs were only located in the edge of the well, however no explanation was found for this event. The control 21% pO_2 group produced a full-well monolayer of CMs. Regarding flow cytometry, CM were identified as cells expressing NKX-2.5 and sarcomeric α-actinin. Overall, a decrease on CM yield was observed in all conditions using the physiological 4% pO_2 levels, compared to the 21% control (movie 3.1-3.2). As expected, pre-conditioned 4% pO_2 condition presented higher yields than differentiations performed at 4% pO_2 and 21% pO_2 only up to D-1. In addition, experiment-to-experiment variation was observed regarding the CM differentiation efficacy.

3.3. Extra in vivo pO_2 condition increased differentiation yield of hESC into CMs.

Differentiated CMs using 4% pO_2 experimental setup, gave the urge to increase the differentiation yield, for that it was stablished two distinct strategies: different hESC seeding densities and extra in vivo pO2 condition (7%). The values chosen for the different hESC seeding densities were based on the previous group experience, which suspected that the results obtained in the first differentiation (26.3 × 10^6 cells/$cm^{2)}$ could be related to over seeding. Hence, CM differentiation was performed using the 4% and 4%2 conditions using six hESC seeding densities ranging from 10.5 × 10^6 cells/cm^2 to 26.3 × 10^6 cells/cm^2 (Figure 3.3.1). The higher seeding densities of 21 × 10^6 cells/cm^2 and 26.3 × 10^6 cells/cm^2 produced better yields of CM differentiation, showing that no protocol alteration was needed. In accordance to our previous results, the experimental group 4% resulted in more CMs than the 4%2, (movies 4-15). However, due to technical problems no flow cytometry was performed on this experiment to quantify the differentiation efficiency/yield.

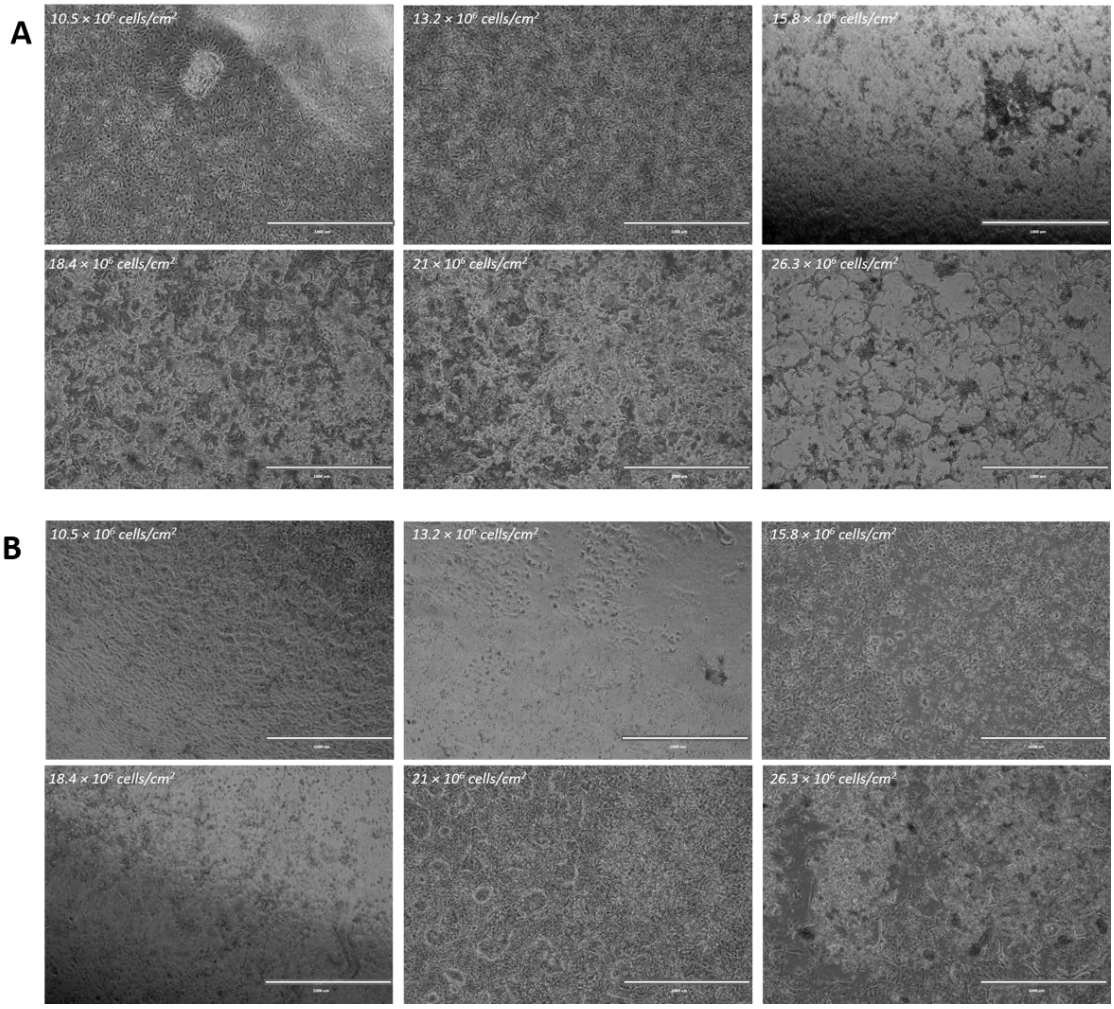

Figure 3.3.1. Representative images of 14 days CM differentiation using 4% (A) and 4%2 conditions (B) and different cell seeding densities. Each image, from left to right and top to bottom, represents hESC increasing densities. Scale bar, 1000µm.

After the third month of gestation is explicit on literature another in vivo pO2 condition (7%)[81] and it was added to increase the differentiation efficiency. In this setup, instead of maintaining the the cells for 14 days at 4% pO_2, they were transferred to an incubator at 7% at day 7 and kept until day 14 in this condition as demonstrated on the scheme (Figure 3.3.3).

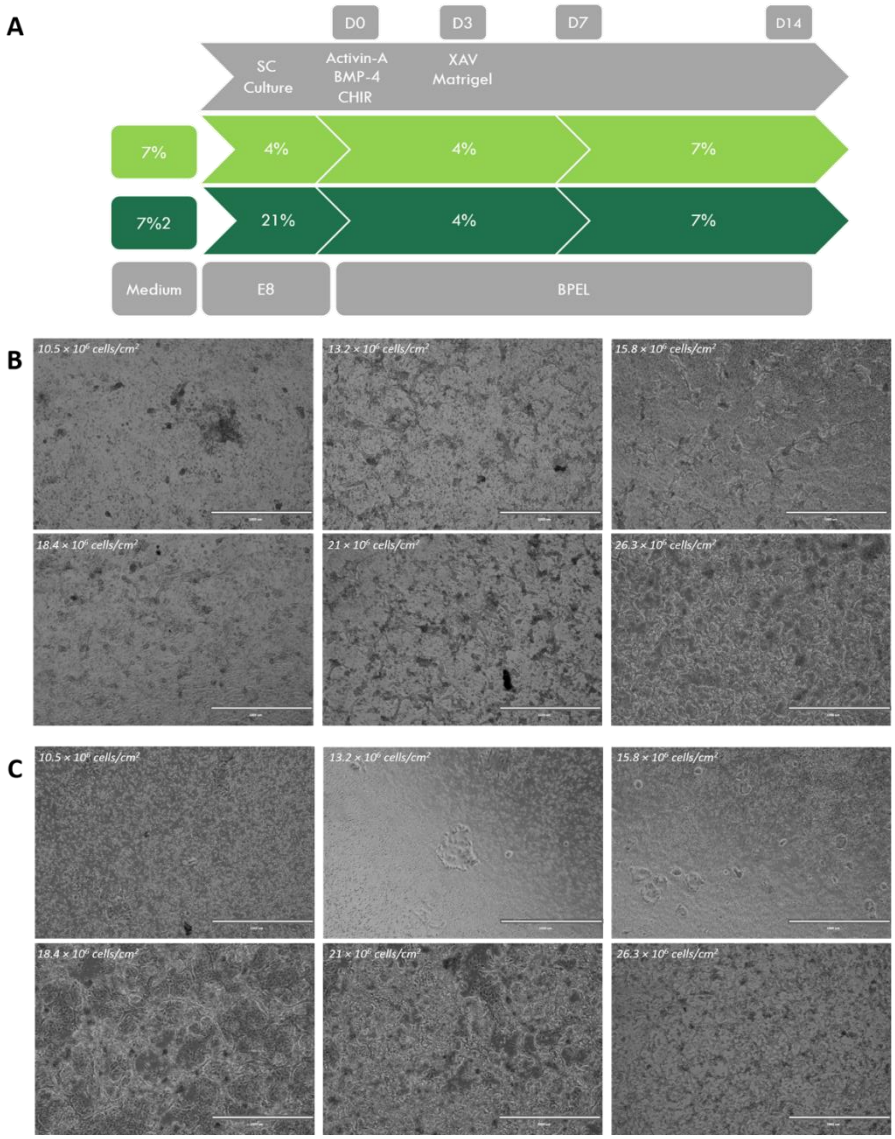

Figure 3.3.2. A- Diagram illustrating experimental physiological pO_2 setup with extra 7% O_2 level, 14-day procedure. 21% group (control), was always kept at all stages under 21% pO2; 7% group originated from 4% SC. 7%2 group have their origin on 21% SC. During differentiation, cells instead of being during 14 days at 4% pO_2 they are placed at 7% pO_2 at day 7 of the experiment. Small grey boxes indicated the day of culture ("D-1", "D0", "D3", "D7" and "D14"). Medium group indicates to what kind of medium cells were cultured, SC stage cultured in E8 and differentiation stage cultured on BPEL. Timeline of differentiation factors added to medium presented on grey arrow. B and C- Representative images of 14 days CM differentiation using 7% (B) and 7%2 conditions (C) and different cell seeding densities. Each image, from left to right and top to bottom, represents hESC increasing densities. Scale bar, 1000µm.

To evaluate if different seeding densities would have an impact on CM differentiation using this setup (conditions 7% and 7%2), different cells densities were used as in the previous experiment.

Once again, the different seeding densities showed that no protocol alteration was needed, since seeding densities of 21 × 10^6 cells/cm^2 and 26.3 × 10^6 cells/cm^2, which were already being used during experiments, showed better results. It was also observed that once again the experimental group that uses 4% during hESC maintenance provided more CMs (Figures 3.3.2. and movies 16-27)).

To further quantify and compare CM yields under embryonic physiological oxygen tension with the conventional 21% group, flow cytometry was performed.

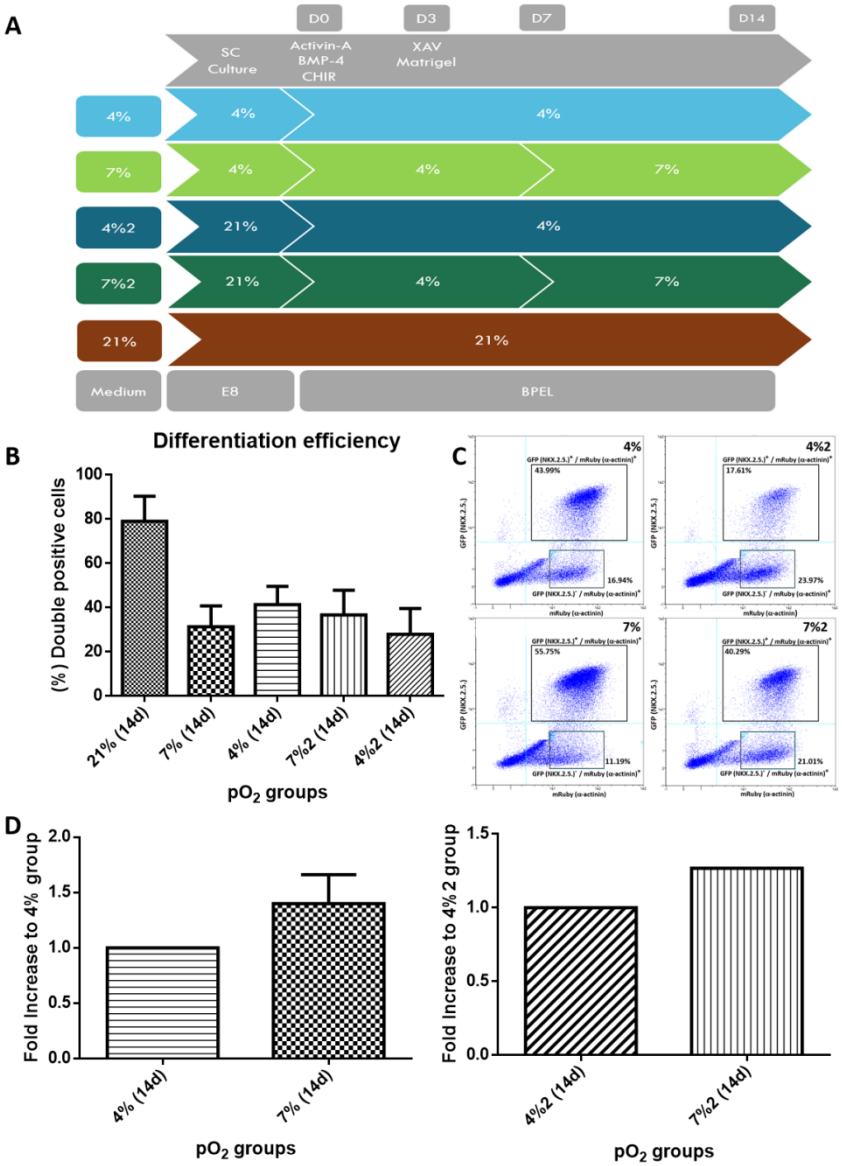

Figure 3.3.3. A- Diagram illustrating complete experimental **physiological** pO_2, 14-day procedure. 21% group (control), was always kept at all stages under 21% pO2; 4% group originated from 4% SC. 4%1 and 4%2 group have their origin on 21% SC. 4% group was always kept at all stages under 4% pO2, while 4%2 group was kept at this condition for 14 days. 7% group originated from 4% SC. 7%2 group have their origin on 21% SC. During differentiation, cells instead of being during 14 days at 4% pO2 they are placed at 7% pO2 at day 7 of the experiment. Small grey boxes indicated the day of culture ("D-1", "D0", "D3", "D7" and "D14"). Medium group indicates to what kind of medium cells were cultured, PSC stage cultured in

E8 and differentiation stage cultured on BPEL. Timeline of differentiation factors added to medium presented on grey arrow. B- Different group differentiation efficiency of hESC derived CMs analysed through flow cytometry. The cells are divided per differentiation group. Control-21% group, 7%group, 4% group, 7%2 group and 4%2 group. Results presented as percentage (%) of cells GFP (NKX 2.5)+/mRuby (α-actinin)+ characteristic of CMs. Bars represent SEM.*P<0.05 vs Control, T-Test was used for all the parameters presented. C- Flow cytometry analysis of different experimental groups. Gating for GFP-NKX2.5. (y axis) and mRuby- α -actinin (x axis). Percentage related to to the two existing population GFP (NKX 2.5)+/mRuby (α -actinin)+ and GFP (NKX 2.5)-/mRuby (α -actinin)+. At least 60 × 106 cells were analysed per group. D- Represent impact of 7% pO2 condition on differentiation yield through fold increase 7%vs4% and 7%2 vs 4%2.

Flow cytometry once more evidenced the variability regarding differentiation efficiency obtained between experiments as demonstrated by big error bars. CM differentiation under conventional 21% pO_2 was evidently more robust when compared to the other groups (Figure 3.3.3 B). In addition, the 7% (movie 30) and 7%2 (movie 31) conditions were not able to improve the differentiation outcome, when compared to the 4% (movie 28) and 4%2 groups (movie 29) . Of interest, the insurgence of a second population GFP (NKX 2.5)$^-$/mRuby (α -actinin)$^+$ that may be impacting the final outcome of the differentiations was evident in flow cytometry analysis (Figure 3.3.3C). This population, that expresses the CM marker α-actinin but shows no detectable levels of NKX2.5., has been previously described as a cardiac pacemaker-like population[121].

Since variability on CM differentiation was observed across experiments, and the analysis from in Figure 3.3.3 B results from 3 independent experiments, we hypothesized that this variability may be masking differences across groups. Hence, to further understand the impact of the 7% condition we analysed the fold increase in CMs, relative to the equivalent 4% pO_2 groups, per experiment (Figure 3.3.3. D). This analysis revealed an increment of ~1.5-fold in the 7% condition, when compared to the 4% group, and an increase of ~1.3 in the 7%2 group, relative to the 4%2. Although, the number of independent experiments is limited, especially regarding the 7%2 (n=1), the 7% pO_2 strategy improved the CM differentiation in 5 independent experiments.

3.4. Differentiation of hESC into CMs using embryonic pO_2 levels affects expression of metabolic- and contraction-associated genes.

Since previous studies have reported that hPSC-CM resemble human fetall-CM based on gene expression[122] we assessed the degree of CM maturity generated under physiological O_2 tension, relative to the standard 21%pO_2 group. The expression of a set of genes related to metabolism, in particular glucose transport (PGC-1α, PDK1, LDHB, HADHB, GLUT-1, GLUT-4, HK1, HK2) and fatty acid handling (CPT-1β and PPARα), as well as genes related to CM contraction

such as calcium handling genes (PLN and SERCA2) and contraction apparatus (MYH6, MYH7 and MYBPC3), was evaluated by q-PCR at differentiation day 14.

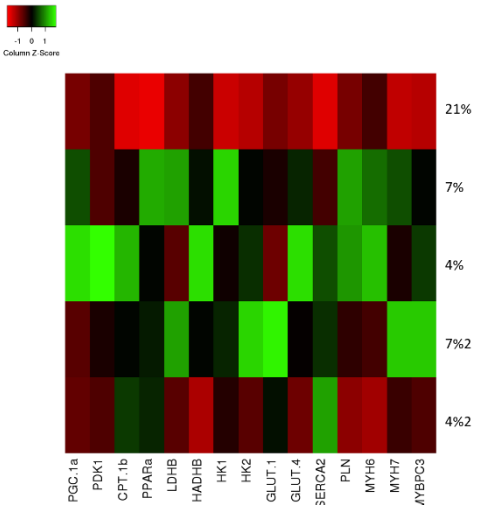

Figure 3.4.1. Heatmap expression of genes encoding metabolic glucose transporters (GLUT-1, GLUT-4, HK1, HK2, HADHB, LDHB, PDK1), metabolic fatty acid mediators (PPARα, CPT-1β), sarcomeric proteins (MYH6, MHY7, MYBPC3), calcium handling channels (PLN, SERCA2) and the mitochondrial master regulator PGC1α. Data was normalized to RPLP expression and is related to the 21% (14d) group. From all the group condition $3 \leq n \leq 5$.

The heatmap demonstrated that overall gene expression is different in 7%, 4% and 7%2 groups, when compared to 21% pO_2 was altered (Figure 3.4.1.). In contrast, the 4%2 group gene expression resembles more the 21% condition regarding the expression of the analysed genes.

The heatmap also reveal that PGC-1α, a mediator of the transition from the glycolytic metabolism to OXPHOS metabolism, has increased expression on 4% and 7%, relative to the other culture conditions (Figure 3.4.1). For this reason, from this point onwards we proceeded only with condition 4% and 7%.

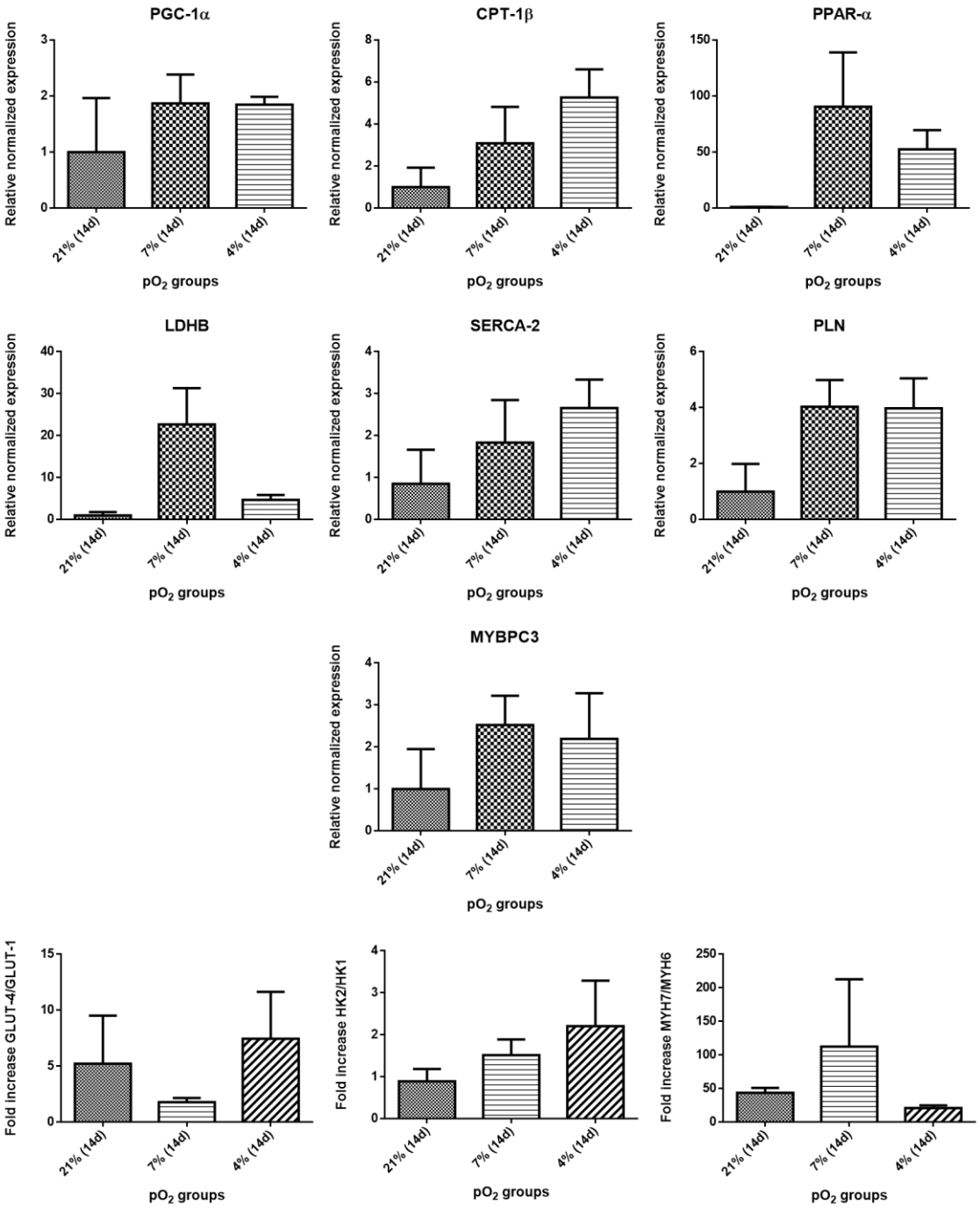

Figure 3.4.2. qPCR gene expression analysis of day 14 of CM differentiation in conventional (21%) and embryonic O_2 tension (7% and 4%). Graph bars represent fold increase relative to the 21% group after normalization to the RPLP0 housekeeping gene. Data are expressed as mean ± SEM. Data was obtained from 3 independent experiments.

Glucose transport metabolic associated genes such as LDHB, HK1, HK2, GLUT-4 presented an increase expression while PDK1, HADHB and GLUT-1 the expression was not altered comparing to control.

Fatty acid metabolic genes CPT-1α and PPARα and calcium handling genes PLN and SERCA2 were increased in 7% and 4% groups, relative to 21% (Figure 3.4.1.). Contractile machinery genes related to the myosin heavy chain unit, MYH7 and MYBPC3, revealed augmented expression while MYH6 kept stable (Figure 3.4.1.). To further understand whether physiological O2 tension is resulting in CMs on a more mature stage, we analysed the ratio of genes related to different stages of CM development. For example, higher expression of GLUT-1, HK1 and MYH6 are related to a more immature stage, while higher expression of GLUT-4, HK2 and MYH7 correlates to a more mature CM.

3.5. Differentiation of hESC into CMs using embryonic pO_2 levels does not impact on mitochondria spatial localization.

During metabolic maturation, mitochondria increase in number, through an equilibrium of fusion and fission [123], increase invagination of membranes and align with CM sarcomeres by migrating from the perinuclear area. To understand whether CMs differentiated in physiological O_2 tension show mitochondrial alterations compatible with CM maturation, we co-stained the nucleus, sarcomeric α-actinin and mitochondria. No substantial differences were found between experimental groups on mitochondria localization. Of note, binuclear cells were found on the 4% and 7% group, compared to the 21% control.

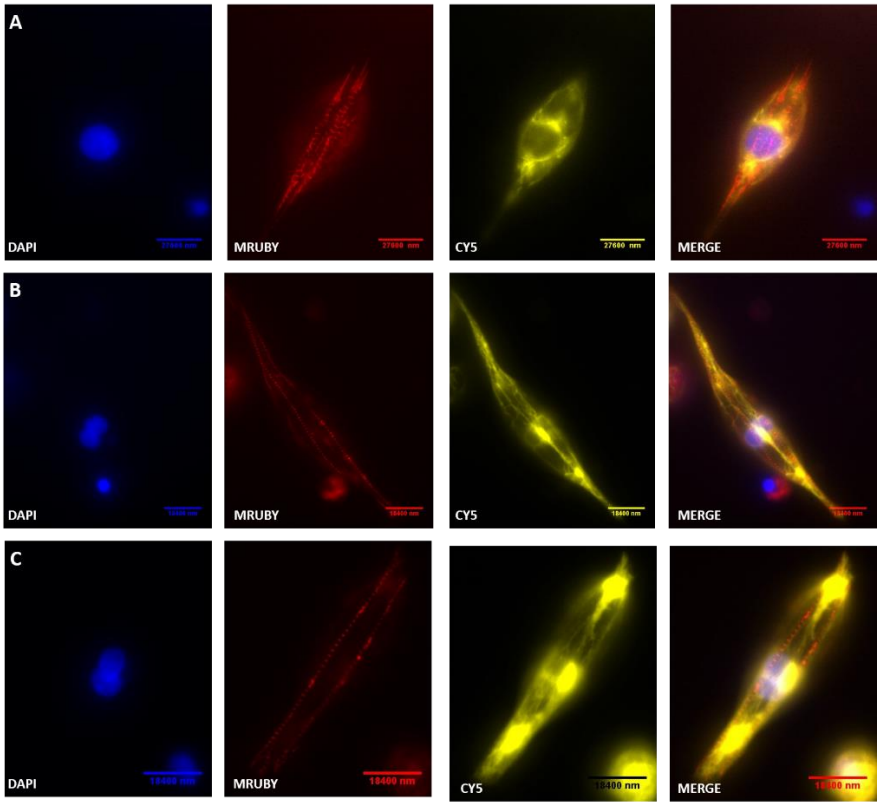

Figure 3.5.1. Representative images of sarcomeres (α-actinin, MRUBY) and mitochondria (CY5) of differentiated CM using embryonic 4% (B) and 7% (C) pO2 levels, relative to 21% (A) control condition. Scale bar represent 27600 (A) 18440 nm (B and C).

3.6. Simulation of birth O_2 tension on differentiated CMs affects gene expression of genes associated with CM metabolic and contraction.

Afterbirth, the neonate starts to breath independently and the diet is also changed, greatly impacting on the maturation of the heart. In line with this, we designed a new experimental procedure to simulate this "birth shock" *in vitro*. For that an O2 tension of 10% was introduced at day 14 of culture until day 21. Substrate-wise, to mimic *in vivo* physiology we used a CM medium supplemented with 5mM glucose (Glc) and 30mM fatty acids (FA) (linoleic acid). A schematic representation of all the tested conditions is summarized in Figure 3.6.1.

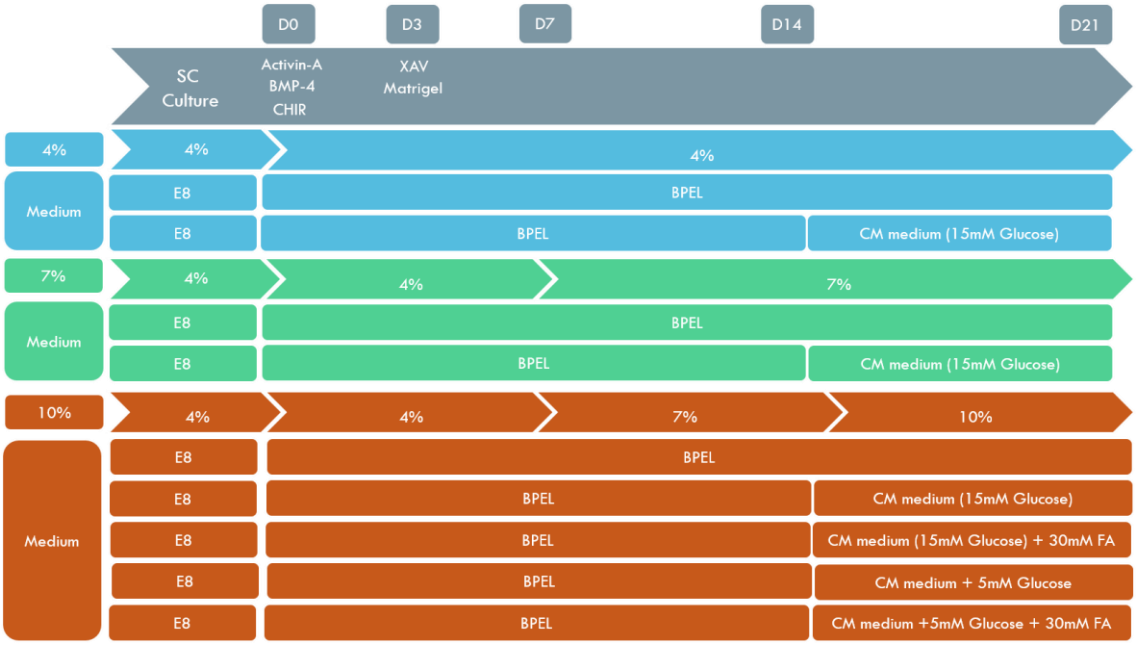

Figure 3.6.1. Diagram illustrating experimental setup designed to drive CMs under physiological oxygen tensions and specifically, to promote the impact of "birth shock" (increase of oxygen tension, as well introduction to physiological glucose and fatty acids levels). The 4% group (blue colour) either with the BPEL medium for the 21 days and the BPEL medium until day 14 plus CM medium for the final 7 days. The 7% group (green colour) either with the BPEL medium for the 21 days and the BPEL medium until day 14 plus CM medium for the final 7 days. In the 10% group (orange colour) we tested the CM medium with 5mM Glucose and 30mM FA as the ideal and final condition. The remaining subgroups of 10% are controls of medium conditions.

Gene expression analysis of the panel of genes related to metabolism and CM contraction studies in previous experiments further highlighted cultured conditions driving CM maturation (Figure 3.6.2).

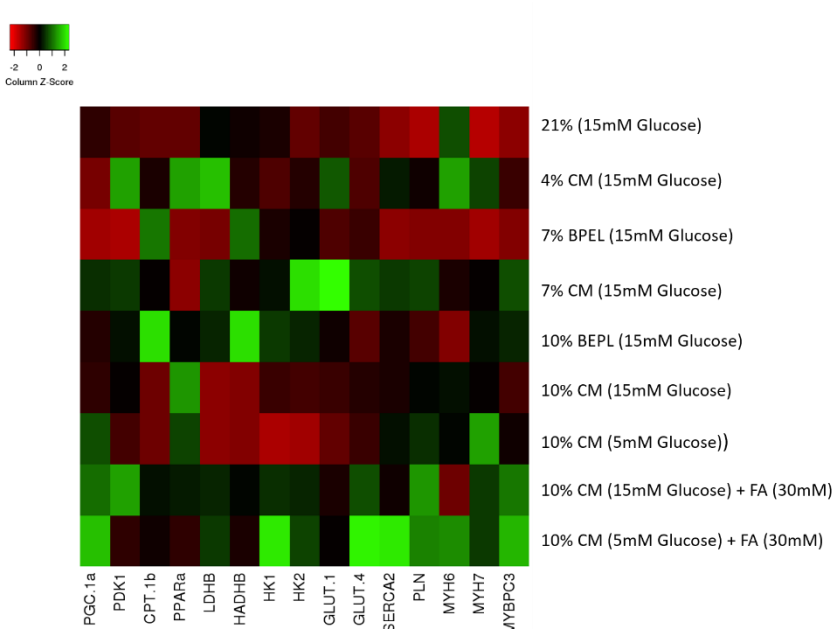

Figure 3.6.2. Heatmap expression of genes encoding metabolic glucose transporters (GLUT-1, GLUT-4, HK1, HK2, HADHB, LDHB, PDK1), metabolic fatty acid mediators (PPARα, CPT-1β), sarcomeric proteins (MYH6, MHY7, MYBPC3), calcium handling channels (PLN, SERCA2) and the mitochondrial master regulator PGC1α. Data was normalized to RPLP expression and is related to the 21% (14d) group. From all the group condition $3 \leq n \leq 5$.

Overall, the "birth shock" experimental setup (10% pO_2 with Glc and FA) resulted on dramatic changes on gene expression compared to the standard 21% group (Figure 3.6.2 and 3.6.3). The 10% pO_2 with Glc and FA experimental subgroup showed increased expression of PGC-1, of the glucose transport metabolic genes HK2 and GLUT-4 and the calcium handling genes PLN and SERCA2. Contractile machinery genes related to the myosin heavy chain unit, MYH7 and MYBPC3, also revealed augmented expression while MYH6 was decreased (Figure 3.6.2 and 3.6.3). The expression ratio of genes related to different stages of CM development also demonstrated a generalized fold increase in CM maturation-related genes in the 10% pO_2 with Glc and FA group, compared to standardized 21% group.

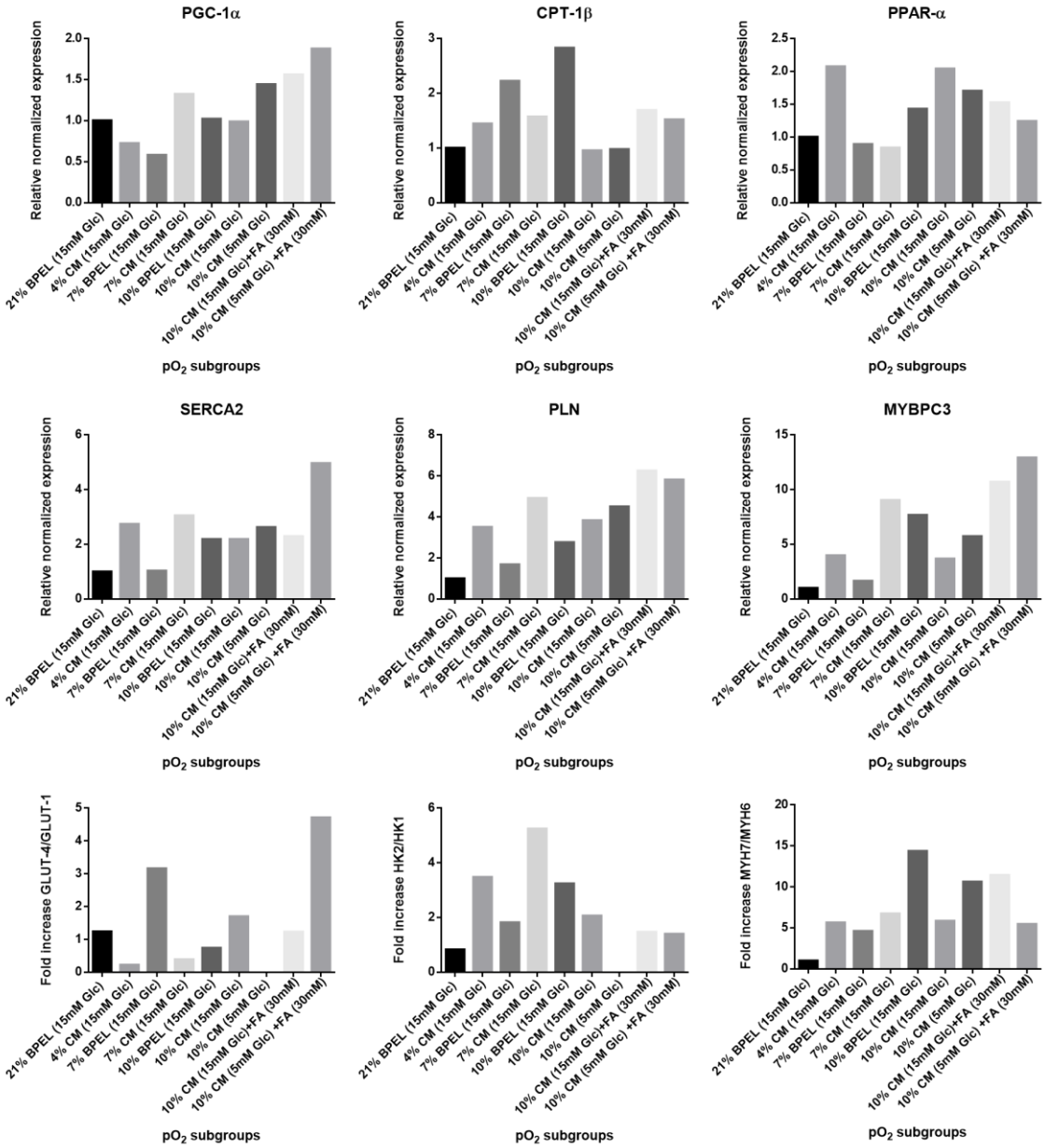

Figure 3.6.3. qPCR gene expression analysis of day 21 of CM differntiation in conventional (21%) and embryonic O_2 tension (7% and 4%). Graph bars represent fold increase relative to the 21% group afternormalization to the RPLP0 housekeeping gene. Data are expressed as mean ± SEM .data was obtained from 1 independent experiments.

3.7. Simulation of birth O_2 tension on differentiated CMs increases the number of mitochondria.

Mitotracker detection by flow cytometry allowed the asessement of mitochondria development i.e. more signal intensity correlates with more mitochondria in the cell.

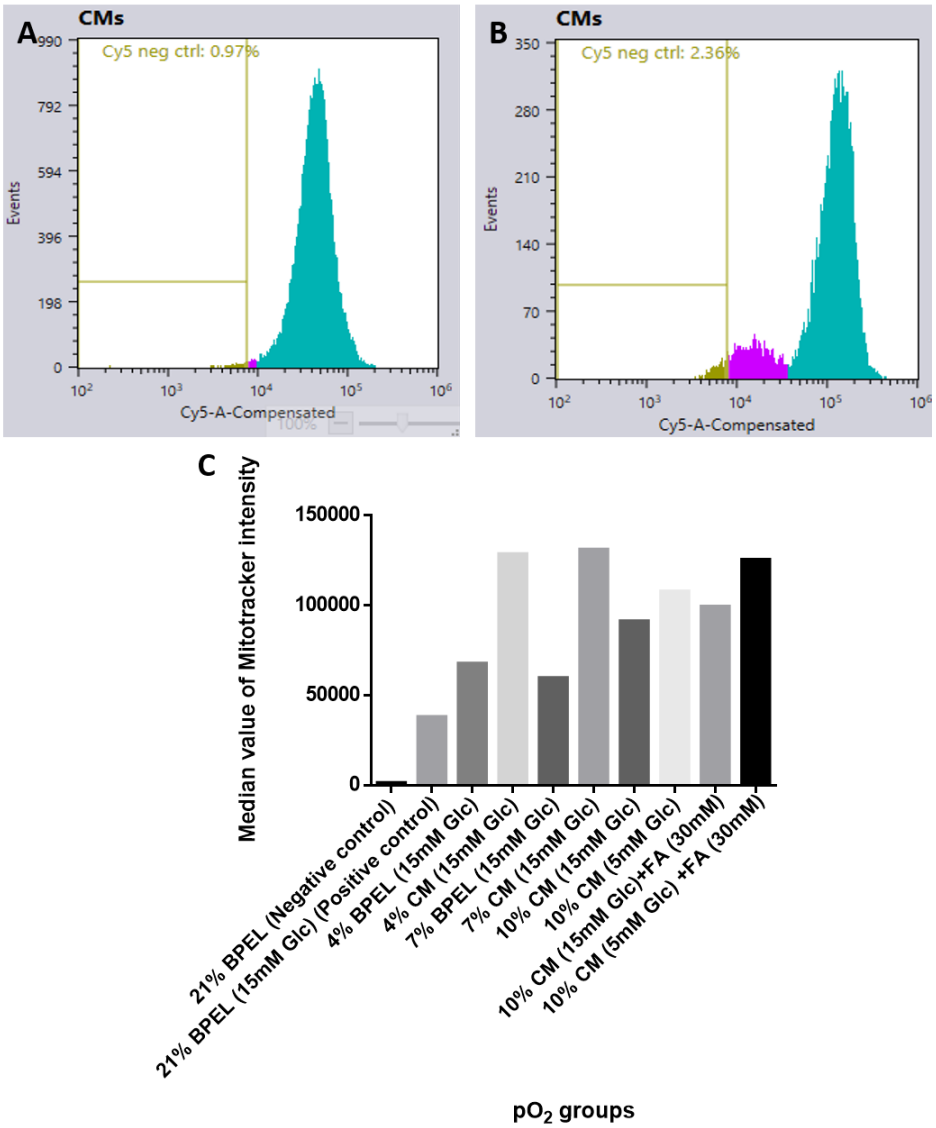

Figure 3.7.1. Mitochondria quantification per experimental subgroup. Histograms show M-labeled cells (gated based on GFP expression) in the 21% and 10% CM + Glc (5mM) + FA (30mM) groups. At least 10,000 cells were analysed per group. C) Graph bar showing the median Mitotacker intensity per pO2 subgroup. Negative control - CMs from the 21% group without Mitotracker; Positive control- CMs from the 21% group stained with Mitotracker.

Flow cytometry analysis of the Mytotracker revealed existence of a two CMs population with two discrete Mitotracker intensity signals (Figure 3.7.1.). The impact of “birth shock” experiment in mitochondria development was evaluated through the calculation of median intensity

value per experimental subgroup (Figure 3.7.2.). At 4% and 7% group, the cells culture on CM medium presented higher median intensity, while in the 10% group no differences were detected between the two media. All subgroups showed substantial difference to control.

3.8. hESC derived CMs seeding and maintenance on a I/R disease model chip.

Microfluidic chips contain small volumes, they have high internal resistances, applying very small variations in temperature and medium solute concentrations that affect the inherent cell behaviour. Aiming at the development of a IR chip with CM for robust in vitro studies, we optimized the seeding of CMs on a chip. Microscopy inspection of the cells through time revealed discrete phenotypic changes. Initially, CMs attached and formed colonies that started beating around day 2 (figure 3.8.1.B, movie 32-33). Then CMs formed bigger beating colonies. However, from day 5 onwards(figure 3.8.1.C, movie 34), colonies started to shrink and CM started to die (Figure 3.8.1.). The intended objective was to keep a confluent monolayer of CM on I/R chip for further studies, what revealed the need of using high seeding densities between approximately 3 x 10^6 cells/cm^2 and 8 x 10^6 cells/cm^2 and medium refreshment every 2 to 3 days. CMs could produce a compact monolayer with several colonies beating observable on bright field and fluorescence α-actinin linked videos of figure 3.8.1. Equal seeding density was achieved in every channel.

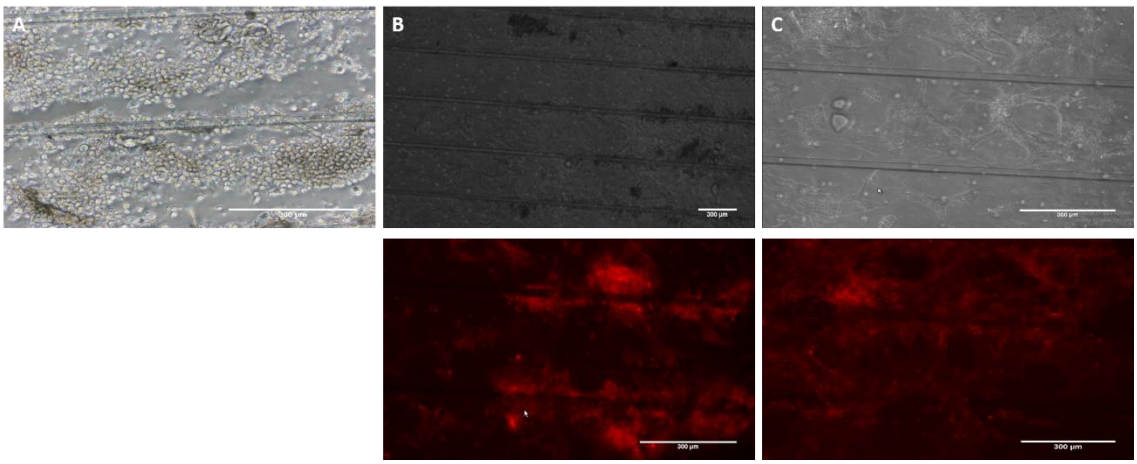

Figure 3.8.1. Imaging of organ-on-a-chip I/R model CMs maintenance using bright field and fluorescence m-Ruby α-actinin microscopy. A) Day zero bright field microscopy B) Third day bright field and fluorescence microscopy C) Fifth day bright field and fluorescence microscopy. Scale bar, 300µm.

3.9. Mechanical stimulation chip, hESC derived CMs seeding and maintenance optimization.

Cells react to the mechanical stimuli input from the surrounding cells and tissues and CMs, in particular, are cells under constant mechanical stress. To understand the impact mechanical stimuli on hESC derived CMs, the latter were cultured on an organ chip[124] capable of producing cell straining through a malleable membrane, on the pillars area. Following CM seeding Microscopy examination of the CMs through time revealed a heterogeneous cell density along the entire chip (figure 3.9.1. A, movie 35), at day one there is evident cell decreasing from the channel closer to the inlet where the CMs seeding was done. Also CMs that could form contractile structures were not aligned on the pillars, area where the stretching of the membranes occurs applying the forces to the cells (Figure 3.9.1.C, movie 37).

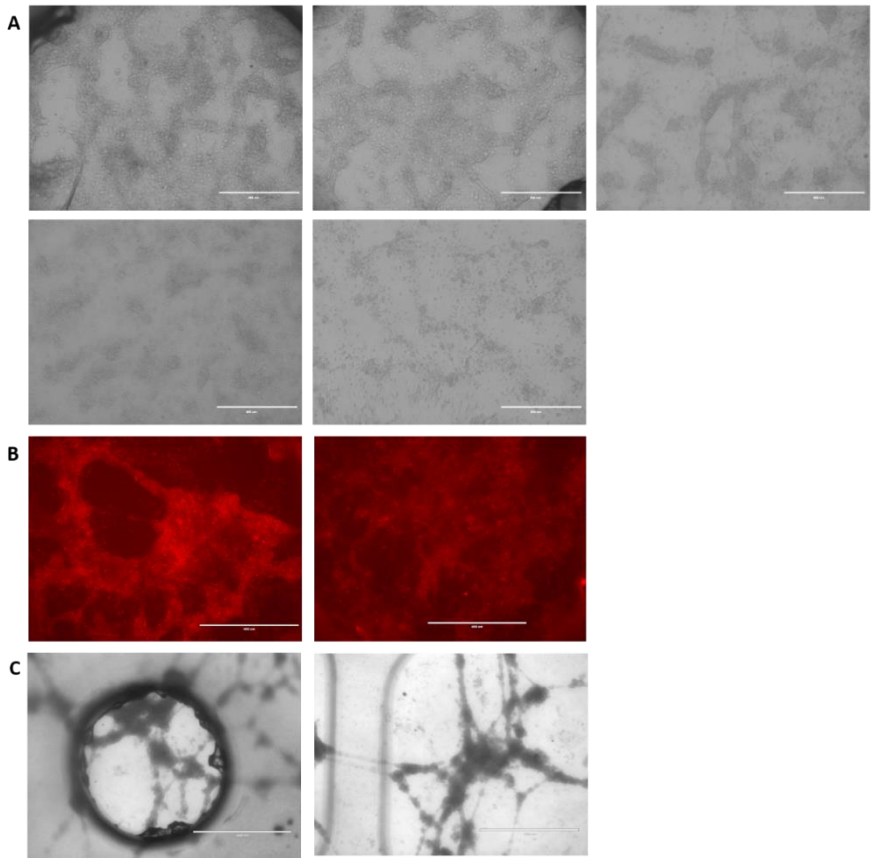

Figure 3.9.1. Imaging of organ-on-a-chip mechanical model CMs maintenance using bright field and fluorescence m-Ruby α-actinin microscopy. A) Day one from left to right, channel 1 to channel 5, bright field microscopy B) Day one (left image) day two (right image)fluorescence microscopy (movie 36) C) Sixth day, pillar with CMs (left image) channels with CMs (right image) bright field microscopy. Scale bar, 300µm (A and B), 100µm (C).

4. Discussion

The initial idea of this project was to recreate an ischemia reperfusion model on an organ-on -a-chip device. However, hESC derived CMs showed an immature phenotype which impaired the development of a model that could reproduce with fidelity the disease scenario. For this reason, this master thesis project was mainly devoted to improve the maturation of hESC-derived CMs that could then be used for appropriate ischemia reperfusion modelling. Accordingly, this thesis project aimed to deliver proof of principle results showing that the use of physiological O_2 tension impacts on the differentiation of CM from hESC, by driving CMs into a more mature stage. In line with this, we envisaged to recreate *in vitro* the final stage of CM maturation mimicking the impact of birth on CMs. For that, we selected two main alterations observed around birth i.e. the increase on O_2 levels, as a result of the beginning of independent air breathing, and the change on the diet, characterized by an increase on fatty acids and decrease on sugars. To ultimately recreate the "birth shock" *in vitro* by rising O2 levels, CM differentiation was firstly established in hypoxic conditions. So the first challenge of this work was to produce hESC colonies at 4% pO2, an O2 tension that mimicked the embryonic cardiac environment. The second challenge, was to differentiate hESC into CMs also using the 4% pO2 condition. The latter was accomplished but with less differentiation efficiency compared to controls. Introducing 7% groups increased differentiation yield.

At this point, flow cytometry analysis showed existence of two cardiac cell populations, ventricular CMs (GFP (NKX 2.5)+/mRuby (α-actinin)+), and a GFP (NKX 2.5)-/mRuby (α-actinin)+ population, most likely a pacemaker-like cell population . This goes in line with the development of the heart, in which pacemakers and myocardial working-CM derive from a common developmental precursor.[121]. Differentiation of cells from a SC population is a biological process technically demanding, in which differentiation efficacy can diverge greatly across experiments. Using our protocol, we obtained a heterogeneous population on control group with CMs but also non-expression cells for NKX2.5 and α-actinin, most likely fibroblasts and other mesodermal lineage cells. These populations, could have impacted the gene expression of our samples, since expression analysis was performed in the entire population at day 14. Hence, our gene expression results provided an indicative and comparative result rather than a direct assessment of the maturation status. Gene study of the FACS-sorted CMs population, using the fluorescent reporters, would have been ideal, however was not possible in time-frame of this project. Relative to standard 21% pO_2 culture conditions, alteration on gene expression were observed using embryonic O_2 tension towards the differentiation of more mature CMs. Indeed, upregulation o PPGC-1a, GLUT-4, MYH7, SERCA2 and PLN and downregulation of MYH6, which we observe using physiologic O_2, has been associated by Ronaldson-Bouchard [125] with CM

maturity, while using mechanical and electrical stimuli to drive CM maturation. We observed upregulation on PGC-1α[126], driving CMs into a OXPHOS metabolism, fatty acid nuclear signal transducer (PPAR-α) and mitochondrial transporter (CPT-1b) in 4% and 7% group, compared to 21% pO2. Contractile system also revealed a tendency for improved maturation with increase expression of calcium handling genes, SERCA2 and PLN, giving more stable contraction to CMs. The mechanical machinery from the contractile system also revealed a displacement towards an adult-like CM phenotype, revealing a fold increase on the MYH7/MYH6 ratio, particularly on 7% group, and as well an increment on cardiac specific myosin heavy chain MYBPC3, on both groups.

Herein, the ultimate attempt to drive CMs maturation was attained by mimicking birth alteration, namely through an increase in O2 tension (10% pO_2) and supplementation with low glucose and fatty acids. Gene expression on birth shock experiment is only related to one experiment, however, a clear indication of improved CM maturation was obtained and, therefore, a strong investment should be made to increase experimental replicates. Indeed our results are in line with others, which demonstrated that glucose reduction resulted in CM with more α-actinin staining, more mitochondria and higher PLN and MYH7 expression. In the same work, high levels of glucose suppressed the expression of PGC-1α. These findings go in line to what we observe in Figure 3.7.1. where 5mM Glc produce higher median intensity than same condition with 15mM of Glc, in Figure 3.6.3. explicit in the case of PGC1-α. Also accordance to our results, Marc van Bilsen[127], using physiological levels of FA, reported an increment on PPAR-a expression and reduction on HK2 and GLUT-4 ratios. Adding to this John M. Brandt [128] correlated the increase expression of PPARa with the shown increase expression of CPT-1b when cells are exposed to FA.

To unequivocally demonstrate that physiological oxygen tension improves CM maturation, it would be important to increase the number of independent experiments, but also other depth analysis are required, such as transmission electron microscopy and studies on action potential. In addition, time in culture is a fundamental step to achieve greater CMs maturity[129] and many of our analysis were performed at day 14 of differentiation, a few days after the cells start to beat. However, through the use of physiological oxygen tension we were able to observed an important detail of CM maturation, de binucleation of the cell[129], it was only observed on 4% and 7% population (Figure 3.5.1) which advocates CM maturity in our experimental setting.

Mitochondria through development increases in number in response to higher energetic demands from CMs, and also intensifies membrane invagination[130]. Since mitochondrial development is an important feature during metabolic maturation of CMs[130], we analysed mitochondria using Mitotracker, which binds to thiols groups of the mitochondrial membranes. Mitochondria/mitochondrial invagination on 4%, 7% and 10 % groups was higher, relative to the conventional 21% pO2 condition. Also, CM medium is known from group experience (unpublished data) to drive CMs into a more mature state, which was noticeable by comparing 4% and 7% CM

(15mM Glc) subgroups with 4% and 7% BPEL (15mM Glc) with the increased Mitotracker mean intensity.

Regarding the I/R disease model chip, the latter showed suitable properties to maintain CMs even with low medium refreshment comparing to the final using method where will have a continuous flux created by a pump system, providing fresh medium while in normal/reperfusion situation or only providing the flux to the external channel (s) in order to promote the ischemia gradient. In what concerns the mechanical stimuli chip, it needed optimization because of the big surface area of the chip ($56cm^2$), requiring 12 x 10^6 cells for seeding, which enabled further studies in the timeframe of this work. Also , the interconnected channels were not able to provide "multiplexing" of the impact of mechanical stimuli and area of stimuli input was too small (ratio area stimuli/total area). These limitation were reported to the collaboration group which designed the chip, accompanied by some proposals on design alterations.

Overall, this work contributed to demonstrate that O_2 tension during *in vitro* cardiac differentiation impacts on CM maturation and that mimicking physiological O_2 levels and diet may significantly improve the generation of mature CMs *in vitro*, thus, contributing to the generation of robust disease models for high-throughput drug testing.

5. Conclusion

Natural engineering philosophy has proven that is worth the effort to mimic what we observe in the human body, the conjugation of conditions is limitless but firstly, steady individual results should be obtained to narrow our aim to specific conditions and objectvies. Results showed that is possible to obtain CMs using pO_2 values consider wrongly as hypoxic. To obtain hESC-derived CMs is by itself a complex and variable process, using the physiological O_2 conditions increases this variability, leading to urge for protocol optimization. In vivo pO_2 differentiation of hESC-derived CMs, had an impact on gene expression of most genes choosed, in line to what is observed in maturational markers of adult CMs. Simulation of the birth impact also added extra maturational landscape on gene expression and mitochondrial development.

Organ-on-a-chip is revealing to be a breakthrough technology, however a lot of time is needed to develop a single model, where all the conditions to mimic the disease/tissue model with easy manoeuvring and high throughput, demand an exhaustive and detailed work, urging the creation of more interdisciplinary groups to tackle in once all the problems that could appear, biological, mechanical, electronical or chemistry related issues.

References

[1] B. Z. Stanger, "Organ size determination and the limits of regulation," *Cell Cycle*, vol. 7, no. 3, pp. 318–324, 2008.

[2] P. Ahuja, P. Sdek, and R. W. Maclellan, "Cardiac Myocyte Cell Cycle Control in Development, Disease and Regeneration," *Physiol. Rev.*, vol. 87, no. 2, pp. 521–544, 2007.

[3] F. Li, X. Wang, J. M. Capasso, and A. M. Gerdes, "Rapid transition of cardiac myocytes from hyperplasia to hypertrophy during postnatal development," *J. Mol. Cell. Cardiol.*, vol. 28, no. 8, pp. 1737–1746, 1996.

[4] S. D. Vincent and M. E. Buckingham, "How to make a heart. The origin and regulation of cardiac progenitor cells," *Curr. Top. Dev. Biol.*, vol. 90, no. C, pp. 1–41, 2010.

[5] T. Brade, L. S. Pane, A. Moretti, K. R. Chien, and K. L. Laugwitz, "Embryonic heart progenitors and cardiogenesis.," *Cold Spring Harb. Perspect. Med.*, vol. 3, no. 10, pp. 1–17, 2013.

[6] A. Bonci, C. R. Lupica, and M. Morales, "HHS Public Access," vol. 18, no. 3, pp. 386–392, 2015.

[7] D. Montani *et al.*, "Targeted therapies in pulmonary arterial hypertension," *Pharmacol. Ther.*, vol. 141, no. 2, pp. 172–191, 2014.

[8] D. J. Hearse, "Myocardial ischemia: can we agree on a definition for the 21st century," *J. Cardiovasc. Res.*, vol. 28, no. 12, pp. 1737–1744, 1994.

[9] G. X. Yan and a G. Kléber, "Changes in extracellular and intracellular pH in ischemic rabbit papillary muscle.," *Circ. Res.*, vol. 71, no. 2, pp. 460–470, 1992.

[10] C. J. A. van Echteld, J. H. Kirkels, M. H. J. Eijgelshoven, P. van der Meer, and T. J. C. Ruigrok, "Intracellular sodium during ischemia and calcium-free perfusion: A 23Na NMR study," *J. Mol. Cell. Cardiol.*, vol. 23, no. 3, pp. 297–307, 1991.

[11] "8. Inhibition of sodium influx and improved preservation of rat hearts.pdf." .

[12] J. G. van Emous, M. G. Nederhoff, T. J. Ruigrok, and C. J. van Echteld, "The role of the Na+ channel in the accumulation of intracellular Na+ during myocardial ischemia: consequences for post-ischemic recovery.," *J. Mol. Cell. Cardiol.*, vol. 29, no. 1, pp. 85–96, 1997.

[13] M. M. Bersohn, "Sodium pump inhibition in sarcolemma from ischemic hearts," *J. Mol. Cell. Cardiol.*, vol. 27, no. 8, pp. 1483–1489, 1995.

[14] E. Murphy and C. Steenbergen, "Mechanisms Underlying Acute Protection From Cardiac Ischemia-Reperfusion Injury," *Physiol. Rev.*, vol. 88, no. 2, pp. 581–609, 2008.

[15] M. Lazdunski, C. Frelin, and P. Vigne, "The sodium/hydrogen exchange system in cardiac cells: Its biochemical and pharmacological properties and its role in regulating internal concentrations of sodium and internal pH," *J. Mol. Cell. Cardiol.*, vol. 17, no. 11, pp. 1029–1042, 1985.

[16] A. P. Halestrap, "Mitochondria and reperfusion injury of the heart-A holey death but not beyond salvation," *J. Bioenerg. Biomembr.*, vol. 41, no. 2, pp. 113–121, 2009.

[17] K. A. Reimer, R. B. Jennings, and A. H. Tatum, "Pathobiology of acute myocardial ischemia: Metabolic, functional and ultrastructural studies," *Am. J. Cardiol.*, vol. 52, no. 2, pp. 72–81, 1983.

[18] J. H. Gilmore, "NIH Public Access," *North*, vol. 29, no. 10, pp. 1883–1889, 2008.

[19] L. Cox, L. Umans, F. Cornelis, D. Huylebroeck, and A. Zwijsen, "A broken heart: A stretch too far. An overview of mouse models with mutations in stretch-sensor components," *Int. J. Cardiol.*, vol. 131, no. 1, pp. 33–44, 2008.

[20] J. C. Rüegg, "Cardiac contractility: How calcium activates the myofilaments," *Naturwissenschaften*, vol. 85, no. 12, pp. 575–582, 1998.

[21] M. L. Srikanth and K. H. McKinlay, "Cardiac excitation???contraction coupling," *Core Top. Card. Anesth. Second Ed.*, vol. 415, no. January, pp. 13–17, 2012.

[22] T. A. Rando, "Stem cells, ageing and the quest for immortality," *Nature*, vol. 441, no. 7097, pp. 1080–1086, 2006.

[23] I. G. M. Brons *et al.*, "Derivation of pluripotent epiblast stem cells from mammalian

embryos," *Nature*, vol. 448, no. 7150, pp. 191–195, 2007.
[24] P. J. Tesar *et al.*, "New cell lines from mouse epiblast share defining features with human embryonic stem cells," *Nature*, vol. 448, no. 7150, pp. 196–199, 2007.
[25] C. L. Kerr, M. J. Shamblott, and J. D. Gearhart, "Pluripotent Stem Cells from Germ Cells," *Methods Enzymol.*, vol. 419, no. 1999, pp. 400–426, 2006.
[26] J. B. Gurdon, T. R. Elsdale, and M. Fischberg, "Sexually mature individuals of Xenopus laevis from the transplantation of single somatic nuclei," *Nature*, vol. 182, no. 4627, pp. 64–65, 1958.
[27] J. B. Gurdon and D. a Melton, "(review) Nuclear reprogramming in cells.," *Science*, vol. 322, no. 5909, pp. 1811–5, 2008.
[28] R. A. Miller and F. H. Ruddle, "Pluripotent Hybrids Somatic Cell Phosphate Isomerase," vol. 9, no. September, pp. 45–55, 1976.
[29] F. M. Watt and R. R. Driskell, "The therapeutic potential of stem cells," *Philos. Trans. R. Soc. B Biol. Sci.*, vol. 365, no. 1537, pp. 155–163, 2010.
[30] Y. Yoshida and S. Yamanaka, "IPS cells: A source of cardiac regeneration," *J. Mol. Cell. Cardiol.*, vol. 50, no. 2, pp. 327–332, 2011.
[31] P. Gadue, T. L. Huber, P. J. Paddison, and G. M. Keller, "Wnt and TGF-beta signaling are required for the induction of an in vitro model of primitive streak formation using embryonic stem cells," *Proc. Natl. Acad. Sci.*, vol. 103, no. 45, pp. 16806–16811, 2006.
[32] R. C. Lindsley *et al.*, "Mesp1 coordinately regulates cardiovascular fate restriction and epithelial-mesenchymal transition in differentiating ESCs," *Cell Stem Cell*, vol. 3, no. 1, pp. 55–68, 2008.
[33] S. Ueno *et al.*, "Biphasic role for Wnt/beta-catenin signaling in cardiac specification in zebrafish and embryonic stem cells," *Proc. Natl. Acad. Sci.*, vol. 104, no. 23, pp. 9685–9690, 2007.
[34] Z. He *et al.*, "Transduction of *Wnt11* Promotes Mesenchymal Stem Cell Transdifferentiation into Cardiac Phenotypes," *Stem Cells Dev.*, vol. 20, no. 10, pp. 1771–1778, 2011.
[35] R. Li *et al.*, "Human pediatric and adult ventricular cardiomyocytes in culture: assessement of phenotypic changes with passaging," *Cardiovasc Res*, vol. 32, p. 12, 1996.
[36] A. M. Gerdes *et al.*, "Structural remodeling of cardiac myocytes in patients with ischemic cardiomyopathy," *Circulation*, vol. 86, no. 2, pp. 426–430, 1992.
[37] C. García-Pérez, G. Hajnóczky, and G. Csordás, "Physical coupling supports the local Ca2+ transfer between sarcoplasmic reticulum subdomains and the mitochondria in heart muscle," *J. Biol. Chem.*, vol. 283, no. 47, pp. 32771–32780, 2008.
[38] Q. Wang *et al.*, "Department of Biology, University of Iowa, Iowa City, IA 52242 USA; 2 Institute of Physiology, National Defense Medical Center, Taipei, Taiwan, ROC; 3 Department of Cardiology, Children's Hospital Boston, Harvard Medical School, Boston, MA 02115 USA," pp. 2566–2593, 2012.
[39] E. Poon, C. W. Kong, and R. A. Li, "Human pluripotent stem cell-based approaches for myocardial repair: From the electrophysiological perspective," *Mol. Pharm.*, vol. 8, no. 5, pp. 1495–1504, 2011.
[40] K. Dolnikov *et al.*, "Functional Properties of Human Embryonic Stem Cell-Derived Cardiomyocytes: Intracellular Ca $^{2+}$ Handling and the Role of Sarcoplasmic Reticulum in the Contraction," *Stem Cells*, vol. 24, no. 2, pp. 236–245, 2006.
[41] P. J. Reiser, M. a Portman, X. H. Ning, and C. Schomisch Moravec, "Human cardiac myosin heavy chain isoforms in fetal and failing adult atria and ventricles.," *Am. J. Physiol. Heart Circ. Physiol.*, vol. 280, no. 4, pp. H1814–H1820, 2001.
[42] and D. S. H. Xiwei Zheng, Cong Bi, Marissa Brooks, "HHS Public Access," *Anal Chem.*, vol. 25, no. 4, pp. 368–379, 2015.
[43] N. T. Ursem, P. C. Struijk, W. C. Hop, E. B. Clark, B. B. Keller, and J. W. Wladimiroff, "Heart rate and flow velocity variability as determined from umbilical Doppler velocimetry at 10-20 weeks of gestation.," *Clin. Sci. (Lond).*, vol. 95, no. 5, pp. 539–45, 1998.
[44] E. J. Lee, J. Peng, M. Radke, M. Gotthardt, and H. L. Granzier, "Calcium sensitivity and the Frank-Starling mechanism of the heart are increased in titin N2B region-deficient mice," *J. Mol. Cell. Cardiol.*, vol. 49, no. 3, pp. 449–458, 2010.
[45] M. Mollova *et al.*, "Cardiomyocyte proliferation contributes to heart growth in young humans," *Proc. Natl. Acad. Sci.*, vol. 110, no. 4, pp. 1446–1451, 2013.

[46] M. C. Ribeiro *et al.*, “Functional maturation of human pluripotent stem cell derived cardiomyocytes invitro - Correlation between contraction force andelectrophysiology,” *Biomaterials*, vol. 51, pp. 138–150, 2015.
[47] R. F. Wiegerinck *et al.*, “Force frequency relationship of the human ventricle increases during early postnatal development,” *Pediatr. Res.*, vol. 65, no. 4, pp. 414–419, 2009.
[48] H. Yang, T. K. Borg, H. Liu, and B. Z. Gao, “Interactive relationship between basement-membrane development and sarcomerogenesis in single cardiomyocytes,” *Exp. Cell Res.*, vol. 330, no. 1, pp. 222–232, 2015.
[49] D. K. Lieu *et al.*, “Absence of Transverse Tubules Contributes to Non-Uniform Ca $^{2+}$ Wavefronts in Mouse and Human Embryonic Stem Cell–Derived Cardiomyocytes,” *Stem Cells Dev.*, vol. 18, no. 10, pp. 1493–1500, 2009.
[50] S. D. Lundy, W. Z. Zhu, M. Regnier, and M. A. Laflamme, “Structural and Functional Maturation of Cardiomyocytes Derived From Human Pluripotent Stem Cells,” *Stem Cells Dev.*, pp. 1–47, 2012.
[51] C. Mummery, “Differentiation of Human Embryonic Stem Cells to Cardiomyocytes: Role of Coculture With Visceral Endoderm-Like Cells,” *Circulation*, vol. 107, no. >21, pp. 2733–2740, 2003.
[52] M. Snir *et al.*, “Assessment of the ultrastructural and proliferative properties of human embryonic stem cell-derived cardiomyocytes Assessment of the ultrastructural and proliferative properties of human embryonic stem cell-derived cardiomyocytes,” *Am J Physiol Hear. Circ Physiol*, pp. 2355–2363, 2016.
[53] X. Yang, L. Pabon, and C. E. Murry, “Engineering adolescence: Maturation of human pluripotent stem cell-derived cardiomyocytes,” *Circ. Res.*, vol. 114, no. 3, pp. 511–523, 2014.
[54] P. W. Burridge *et al.*, “A universal system for highly efficient cardiac differentiation of human induced pluripotent stem cells that eliminates interline variability,” *PLoS One*, vol. 6, no. 4, 2011.
[55] L. B. Hazeltine *et al.*, “Effects of substrate mechanics on contractility of cardiomyocytes generated from human pluripotent stem cells,” *Int. J. Cell Biol.*, vol. 2012, 2012.
[56] J. M. Weitzel, C. Radtke, and H. J. Seitz, “Two thyroid hormone-mediated gene expression patterns in vivo identified by cDNA expression arrays in rat.,” *Nucleic Acids Res.*, vol. 29, no. 24, pp. 5148–5155, 2001.
[57] T. M. Keaveny, E. F. Morgan, G. L. Niebur, and O. C. Yeh, “Iomechanics of,” pp. 1–25, 2001.
[58] P. J. Schlueter *et al.*, “Gene duplication and functional divergence of the zebrafish insulin-like growth factor 1 receptors.,” *FASEB J.*, vol. 20, no. 8, pp. 1230–1232, 2006.
[59] D. E. Ingber, “Tensegrity: the Architectural Basis of Cellular Mechanotransduction,” *Annu. Rev. Physiol.*, vol. 59, no. 1, pp. 575–599, 1997.
[60] P. Satir, L. B. Pedersen, and S. T. Christensen, “The primary cilium at a glance,” *J. Cell Sci.*, vol. 123, no. 4, pp. 499–503, 2010.
[61] F. J. Alenghat and D. E. Ingber, “Mechanotransduction: All Signals Point to Cytoskeleton, Matrix, and Integrins,” *Sci. Signal.*, vol. 2002, no. 119, p. pe6-pe6, 2002.
[62] J. L. Maître and C. P. Heisenberg, “Three functions of cadherins in cell adhesion,” *Curr. Biol.*, vol. 23, no. 14, pp. 626–633, 2013.
[63] D. A. Goodenough and D. L. Paul, “Gap junctions.,” *Cold Spring Harb. Perspect. Biol.*, vol. 1, no. 1, pp. 1–19, 2009.
[64] M. S. Spach, J. F. Heidlage, R. C. Barr, and P. C. Dolber, “Cell size and communication: Role in structural and electrical development and remodeling of the heart,” *Hear. Rhythm*, vol. 1, no. 4, pp. 500–515, 2004.
[65] D. A. Hooks, M. L. Trew, B. J. Caldwell, G. B. Sands, I. J. LeGrice, and B. H. Smaill, “Laminar arrangement of ventricular myocytes influences electrical behavior of the heart,” *Circ. Res.*, vol. 101, no. 10, pp. 103–113, 2007.
[66] E. A. Schroder, Y. Wei, and J. Satin, “The developing cardiac myocyte: Maturation of excitability and excitation-contraction coupling,” *Ann. N. Y. Acad. Sci.*, vol. 1080, pp. 63–75, 2006.
[67] A. M. Gerdes, “Cardiac myocyte remodeling in hypertrophy and progression to failure,” *J. Card. Fail.*, vol. 8, no. 6 SUPPL., pp. 264–268, 2002.
[68] M. L. McCain and K. K. Parker, “Mechanotransduction: The role of mechanical stress, myocyte shape, and cytoskeletal architecture on cardiac function,” *Pflugers Arch. Eur.*

J. Physiol., vol. 462, no. 1, pp. 89–104, 2011.
[69] C. J. Meyer, F. J. Alenghat, P. Rim, J. H. J. Fong, B. Fabry, and D. E. Ingber, "Mechanical control of cyclic AMP signalling and gene transcription through integrins," *Nat. Cell Biol.*, vol. 2, no. 9, pp. 666–668, 2000.
[70] Y. Gruenbaum, A. Margalit, R. D. Goldman, D. K. Shumaker, and K. L. Wilson, "The nuclear lamina comes of age," *Nat. Rev. Mol. Cell Biol.*, vol. 6, no. 1, pp. 21–31, 2005.
[71] F. Torrent-Guasp *et al.*, "Towards new understanding of the heart structure and function," *Eur. J. Cardio-thoracic Surg.*, vol. 27, no. 2, pp. 191–201, 2005.
[72] D. Desmaële, M. Boukallel, and S. Régnier, "Actuation means for the mechanical stimulation of living cells via microelectromechanical systems: A critical review," *J. Biomech.*, vol. 44, no. 8, pp. 1433–1446, 2011.
[73] M. Jain, "A next-generation approach to the characterization of a non-model plant transcriptome," *Curr. Sci.*, vol. 101, no. 11, pp. 1435–1439, 2011.
[74] J. L. Tan, J. Tien, D. M. Pirone, D. S. Gray, K. Bhadriraju, and C. S. Chen, "Cells lying on a bed of microneedles: An approach to isolate mechanical force," *Proc. Natl. Acad. Sci.*, vol. 100, no. 4, pp. 1484–1489, 2003.
[75] W. H. Zimmermann *et al.*, "Tissue engineering of a differentiated cardiac muscle construct," *Circ. Res.*, vol. 90, no. 2, pp. 223–230, 2002.
[76] T. Ezashi, P. Das, and R. M. Roberts, "Low O2 tensions and the prevention of differentiation of HES cells," *Nat. Methods*, vol. 2, no. 5, p. 325, 2005.
[77] J. A. Mitchell and J. M. Yochim, "Intrauterine oxygen tension during the estrous cycle in the rat: its relation to uterine respiration and vascular activity.," *Endocrinology*, vol. 83, no. 4, pp. 701–705, 1968.
[78] B. S. Richardson and A. D. Bocking, "Metabolic and circulatory adaptations to chronic hypoxia in the fetus," *Comp. Biochem. Physiol. - A Mol. Integr. Physiol.*, vol. 119, no. 3, pp. 717–723, 1998.
[79] L. Liu and M. C. Simon, "Regulation of Transcription and Translation by Hypoxia," *Cancer Biol. Ther.*, vol. 3, no. 6, pp. 492–497, 2004.
[80] S. Qanungo and M. Mukherjea, "Ontogenic profile of some antioxidants and lipid peroxidation in human placental and fetal tissues," *Mol. Cell. Biochem.*, vol. 215, no. 1–2, pp. 11–19, 2000.
[81] E. Jauniaux, A. L. Watson, J. Hempstock, Y. P. Bao, J. N. Skepper, and G. J. Burton, "Onset of maternal arterial blood flow and placental oxidative stress. A possible factor in human early pregnancy failure.," *Am. J. Pathol.*, vol. 157, no. 6, pp. 2111–22, 2000.
[82] D. A. Harris and A. M. Das, "Control of mitochondrial ATP synthesis in the heart.," *Biochem. J.*, vol. 280 (Pt 3, pp. 561–573, 1991.
[83] I. O---, "Heart Muscle : Ultrastructural Studies Visvan Navaratnam Cambridge University Press , Cambridge / New," p. 199, 1987.
[84] J. Piquereau *et al.*, "Mitochondrial dynamics in the adult cardiomyocytes: Which roles for a highly specialized cell?," *Front. Physiol.*, vol. 4 MAY, no. May, pp. 1–13, 2013.
[85] J. J. Lopaschuk GD, "Energy metabolic phenotype of the CM during development, differentiation and postnatal maturation," *J Cardiovasc Pharmacol*, vol. 56, no. 2, pp. 130–140, 2010.
[86] T. Itoi and G. D. Lopaschuk, "The contribution of glycolysis, glucose oxidation, lactate oxidation, and fatty acid oxidation to ATP production in isolated biventricular working hearts from 2-week-old rabbits," *Pediatr. Res.*, vol. 34, no. 6, pp. 735–741, 1993.
[87] S.-B. Ong, A. R. Hall, and D. J. Hausenloy, "Mitochondrial Dynamics in Cardiovascular Health and Disease," *Antioxid. Redox Signal.*, vol. 19, no. 4, pp. 400–414, 2013.
[88] R. Ellen Kreipke, Y. Wang, J. W. Miklas, J. Mathieu, and H. Ruohola-Baker, "Metabolic remodeling in early development and cardiomyocyte maturation," *Semin. Cell Dev. Biol.*, vol. 52, pp. 84–92, 2016.
[89] J. C. Werner and R. E. Sicard, "Lactate metabolism of isolated, perfused fetal, and newborn pig hearts.," *Pediatr. Res.*, vol. 22, no. 5, pp. 552–556, 1987.
[90] S. Chung, P. P. Dzeja, R. S. Faustino, C. Perez-Terzic, A. Behfar, and A. Terzic, "Mitochondrial oxidative metabolism is required for the cardiac differentiation of stem cells," *Nat. Clin. Pract. Cardiovasc. Med.*, vol. 4, no. SUPPL. 1, pp. 60–67, 2007.
[91] G. D. Lopaschuk, J. R. Ussher, C. D. L. Folmes, J. S. Jaswal, and W. C. Stanley, "Myocardial fatty acid metabolism in health and disease," *Physiol Rev.*, vol. 90, no. 1522–1210 (Electronic), pp. 207–258, 2010.
[92] G. Lopaschuk, "The role of fatty acid oxidation in cardiac ischemia and reperfusion,"

Adv. Stud. Med., vol. 4, no. 10 B, pp. 1093–1129, 2004.
[93] A. E. Wentz *et al.*, "Adaptation of myocardial substrate metabolism to a ketogenic nutrient environment," *J. Biol. Chem.*, vol. 285, no. 32, pp. 24447–24456, 2010.
[94] R. May, "Received May," vol. 113, no. 2, pp. 586–591, 1983.
[95] "No Title."
[96] R. H. Knopp *et al.*, "Lipoprotein metabolism in pregnancy, fat transport to the fetus, and the effects of diabetes[1]," *Neonatology*, vol. 50, no. 6, pp. 297–317, 1986.
[97] G. D. Lopaschuk, R. L. Collins-Nakai, and T. Itoi, "Developmental changes in energy substrate use by the heart," *Cardiovasc Res*, vol. 26, no. 12, pp. 1172–1180, 1992.
[98] C. E. Forristal, K. L. Wright, N. A. Hanley, R. O. C. Oreffo, and F. D. Houghton, "Hypoxia inducible factors regulate pluripotency and proliferation in human embryonic stem cells cultured at reduced oxygen tensions," *Reproduction*, vol. 139, no. 1, pp. 85–97, 2010.
[99] R. J. DeBerardinis, J. J. Lum, G. Hatzivassiliou, and C. B. Thompson, "The Biology of Cancer: Metabolic Reprogramming Fuels Cell Growth and Proliferation," *Cell Metab.*, vol. 7, no. 1, pp. 11–20, 2008.
[100] S. C. Kolwicz, S. Purohit, and R. Tian, "Cardiac metabolism and its interactions with contraction, growth, and survival of cardiomyocytes," *Circ. Res.*, vol. 113, no. 5, pp. 603–616, 2013.
[101] C. Montessuit and R. Lerch, "Regulation and dysregulation of glucose transport in cardiomyocytes," *Biochim. Biophys. Acta - Mol. Cell Res.*, vol. 1833, no. 4, pp. 848–856, 2013.
[102] M. G. Vander Heiden, L. C. Cantley, and C. B. Thompson, "Understanding the warburg effect: The metabolic requirements of cell proliferation," *Science (80-.).*, vol. 324, no. 5930, pp. 1029–1033, 2009.
[103] G. Pourmand *et al.*, "EPCA2.22: A silver lining for early diagnosis of prostate cancer," *Urol. J.*, vol. 13, no. 5, pp. 2845–2848, 2016.
[104] E. T. Kase *et al.*, "Remodeling of Oxidative Energy Metabolism by Galactose Improves Glucose Handling and Metabolic Switching in Human Skeletal Muscle Cells," *PLoS One*, vol. 8, no. 4, 2013.
[105] R. Rossignol, R. Gilkerson, R. Aggeler, K. Yamagata, S. J. Remigton, and R. A. Capaldi, "Energy substrate modulates mitochondrial structures and oxidative capacityin cancer cells," *Cancer Res.*, vol. 64, pp. 985–993, 2004.
[106] C. Aguer *et al.*, "Galactose enhances oxidative metabolism and reveals mitochondrial dysfunction in human primary muscle cells," *PLoS One*, vol. 6, no. 12, 2011.
[107] J. Reitzer and M. Wice, "Is the Major," vol. 254, no. 8, 1979.
[108] R. Zhu, A. Blazeski, E. Poon, K. D. Costa, L. Tung, and K. R. Boheler, "Physical developmental cues for the maturation of human pluripotent stem cell-derived cardiomyocytes.," *Stem Cell Res. Ther.*, vol. 5, p. 117, 2014.
[109] D. Huh, Y. Torisawa, G. A. Hamilton, H. J. Kim, and D. E. Ingber, "Microengineered physiological biomimicry: Organs-on-Chips," *Lab Chip*, vol. 12, no. 12, p. 2156, 2012.
[110] J. Kimmelman and C. Federico, "Consider drug efficacy before first-in-human trials," *Nature*, vol. 542, no. 7639, pp. 25–27, 2017.
[111] J. A. DiMasi, H. G. Grabowski, and R. W. Hansen, "Innovation in the pharmaceutical industry: New estimates of R&D costs," *J. Health Econ.*, vol. 47, pp. 20–33, 2016.
[112] J. A. Eisen, E. Ganley, and C. J. Maccallum, "Open Science and Reporting Animal Studies : Who ' s Accountable ?," *PLoS Biol.*, vol. 12, no. 1, pp. 1–3, 2014.
[113] K. M. Giacomini, S. Huang, Tweedie DJ, and L. Z. Benet, "NIH Public Access," *Nature*, vol. 9, no. 3, pp. 215–236, 2012.
[114] Centers for Disease Control and Prevention, "Heart Disease," 2017.
[115] A. D. van der Meer and A. van den Berg, "Organs-on-chips: breaking the in vitro impasse," *Integr. Biol.*, vol. 4, no. 5, p. 461, 2012.
[116] S. N. Bhatia and D. E. Ingber, "Microfluidic organs-on-chips," *Nat. Biotechnol.*, vol. 32, no. 8, pp. 760–772, 2014.
[117] D. Huh, B. D. Matthews, A. Mammoto, M. Montoya-Zavala, H. Yuan Hsin, and D. E. Ingber, "Reconstituting organ-level lung functions on a chip," *Science (80-.).*, vol. 328, no. 5986, pp. 1662–1668, 2010.
[118] H. J. Kim and D. E. Ingber, "Gut-on-a-Chip microenvironment induces human intestinal cells to undergo villus differentiation," *Integr. Biol.*, vol. 5, no. 9, p. 1130, 2013.
[119] E. Westein, A. D. van der Meer, M. J. E. Kuijpers, J.-P. Frimat, A. van den Berg, and J.

W. M. Heemskerk, “Atherosclerotic geometries exacerbate pathological thrombus formation poststenosis in a von Willebrand factor-dependent manner,” *Proc. Natl. Acad. Sci.*, vol. 110, no. 4, pp. 1357–1362, 2013.
[120] Y. Wang, B.-K. Chou, S. Dowey, C. He, S. Gerecht, and L. Cheng, “Scalable expansion of human induced pluripotent stem cells in the defined xeno-free E8 medium under adherent and suspension culture conditions.,” *Stem Cell Res.*, vol. 11, no. 3, pp. 1103–16, 2013.
[121] R. A. Espinoza-Lewis *et al.*, “Shox2 is essential for the differentiation of cardiac pacemaker cells by repressing Nkx2-5,” *Dev. Biol.*, vol. 327, no. 2, pp. 376–385, 2009.
[122] J. Synnergren, C. Ameen, A. Jansson, and P. Sartipy, “Global transcriptional profiling reveals similarities and differences between human stem cell-derived cardiomyocyte clusters and heart tissue,” *Physiol. Genomics*, vol. 44, no. 4, pp. 245–258, 2012.
[123] M. Liesa, M. Palacin, and A. Zorzano, “Mitochondrial Dynamics in Mammalian Health and Disease,” *Physiol. Rev.*, vol. 89, no. 3, pp. 799–845, 2009.
[124] R. Sinha, N. Verdonschot, B. Koopman, and J. Rouwkema, “Tuning Cell and Tissue Development by Combining Multiple Mechanical Signals,” *Tissue Eng. Part B Rev.*, vol. 23, no. 5, p. ten.teb.2016.0500, 2017.
[125] K. Ronaldson-Bouchard *et al.*, “Advanced maturation of human cardiac tissue grown from pluripotent stem cells,” *Nature*, vol. 556, no. 7700, pp. 239–243, 2018.
[126] M. J. Birket *et al.*, “PGC-1α and reactive oxygen species regulate human embryonic stem cell-derived cardiomyocyte function,” *Stem Cell Reports*, vol. 1, no. 6, pp. 560–574, 2013.
[127] K. A. J. M. Van Der Lee *et al.*, “Long-chain fatty acid-induced changes in gene expression in neonatal cardiac myocytes,” vol. 41, 2000.
[128] J. M. Brandt, F. Djouadi, and D. P. Kelly, “Fatty-acids activate transcription of the muscle carnitine palmitoyltransferase-i gene in cardiac myocytes via the peroxisome proliferator-activated receptor-alpha,” *J. Biol. Chem.*, vol. 273, no. 37, pp. 23786–23792, 1998.
[129] G. Olivetti *et al.*, “Aging, cardiac hypertrophy and ischemic cardiomyopathy do not affect the proportion of mononucleated and multinucleated myocytes in the human heart,” *J. Mol. Cell. Cardiol.*, vol. 28, no. 7, pp. 1463–1477, 1996.
[130] M. J. Legato, “Cellular mechanisms of normal growth in the mammalian heart. II. A quantitative and qualitative comparison between the right and left ventricular myocytes in the dog from birth to five months of age,” *Circ. Res.*, vol. 44, no. 2, pp. 263–279, 1979.